



Research Paper

Zika Virus Causes Persistent Infection in Porcine Conceptuses and may Impair Health in Offspring



Joseph Darbellay^{a,1}, Brian Cox^{b,1}, Kenneth Lai^{a,1}, Mario Delgado-Ortega^{a,1}, Colette Wheler^a, Donald Wilson^a, Stewart Walker^a, Gregory Starrak^c, Duncan Hockley^c, Yanyun Huang^d, George Mutwiri^e, Andrew Potter^{a,f}, Matthew Gilmour^g, David Safronetz^g, Volker Gerdtz^{a,f}, Uladzimir Karniychuk^{a,f,e,*}

^a Vaccine and Infectious Disease Organization-International Vaccine Centre (VIDO-InterVac), University of Saskatchewan, Saskatoon, SK S7N 5E3, Canada

^b Department of Physiology, Department of Obstetrics and Gynaecology, University of Toronto, Toronto, ON M5S 1A8, Canada

^c Department of Small Animal Clinical Sciences, Western College of Veterinary Medicine, University of Saskatchewan, Saskatoon, SK S7N 5B4, Canada

^d Prairie Diagnostic Services, Saskatoon, SK S7N 5B4, Canada

^e School of Public Health, University of Saskatchewan, Saskatoon, SK, Canada

^f Department of Veterinary Microbiology, Western College of Veterinary Medicine, University of Saskatchewan, Saskatoon, SK S7N 5B4, Canada

^g Canada National Microbiology Laboratory, Public Health Agency of Canada, 1015 Arlington Street, Winnipeg, MB R3E 3R2, Canada

ARTICLE INFO

Article history:

Received 3 August 2017

Received in revised form 11 September 2017

Accepted 15 September 2017

Available online 21 September 2017

Keywords:

Zika virus

Fetus

Offspring

Persistent infection

Behavior

Pig

ABSTRACT

Outcomes of Zika virus (ZIKV) infection in pregnant women vary from the birth of asymptomatic offspring to abnormal development and severe brain lesions in fetuses and infants. There are concerns that offspring affected *in utero* and born without apparent symptoms may develop mental illnesses. Therefore, animal models are important to test interventions against *in utero* infection and health sequelae in symptomatic and likely more widespread asymptomatic offspring. To partially reproduce *in utero* infection in humans, we directly inoculated selected porcine conceptuses with ZIKV. Inoculation resulted in rapid trans-fetal infections, persistent infection in conceptuses, molecular pathology in fetal brains, fetal antibody and type I interferon responses. Offspring infected *in utero* showed ZIKV in their fetal membranes collected after birth. Some *in utero* affected piglets were small, depressed, had undersized brains, and showed seizures. Some piglets showed potentially increased activity. Our data suggest that porcine model of persistent *in utero* ZIKV infection has a strong potential for translational research and can be used to test therapeutic interventions *in vivo*.

© 2017 The Authors. Published by Elsevier B.V. This is an open access article under the CC BY-NC-ND license (<http://creativecommons.org/licenses/by-nc-nd/4.0/>).

1. Introduction

Outcomes of Zika virus (ZIKV) infection in pregnant women vary from the birth of asymptomatic offspring to abnormal development and severe brain lesions in fetuses and neonates (Brasil et al., 2016b; Krauer et al., 2017; Mlakar et al., 2016; Rasmussen et al., 2016; Schuler-Faccini et al., 2016). Pathology in symptomatic neonates that have been affected *in utero* comprises small-for-gestational-age (SGA) phenotype, lesions in the brain, microcephaly, epilepsy, and altered behavior associated with irritability, impatient crying, and anxiety (Brasil et al., 2016a; Moura da Silva et al., 2016; Rasmussen et al., 2016; van der Linden et al., 2016). The full clinical spectrum of long-term health sequelae in symptomatic individuals has yet to be elucidated. The potential effects of likely more widespread asymptomatic ZIKV infection

in mother and fetus on health in offspring are also not known (Brasil et al., 2016a; Kapogiannis et al., 2017; Rasmussen et al., 2016). The most recent surveillance in the United States territories showed that among completed pregnancies with positive tests confirming ZIKV infection, the percentage of fetuses and infants with ZIKV-associated birth defects was only 4–8% (Shapiro-Mendoza et al., 2017). However, there are concerns that *in utero* affected offspring born without apparent symptoms may develop mental illnesses in later life (Torales and Barrios, 2017). Zika virus-associated cognitive impairment and psychiatric symptoms like anxiety, racing thoughts, and an inability to turn off thoughts have also been reported in an acutely infected adolescent (Zucker et al., 2017). Thus, the development of animal models to test interventions against *in utero* ZIKV infection and sequelae in offspring is of high importance.

Studies on pregnant conventional and immunocompromised mice and nonhuman primates (NHP) confirmed detrimental ZIKV-induced congenital pathology and provided insights into ZIKV pathogenesis (Adams Waldorf et al., 2016; Cugola et al., 2016; Li et al., 2016; Miner et al., 2016; Nguyen et al., 2017; Tang et al., 2016; Vermillion et al., 2017; Xavier-Neto et al., 2017). However, studies of health sequelae of

* Corresponding author at: Vaccine and Infectious Disease Organization, International Vaccine Centre (VIDO-InterVac), University of Saskatchewan, Saskatoon, SK S7N 5E3, Canada.

E-mail address: u.karniychuk@usask.ca (U. Karniychuk).

¹ These authors contributed equally.

congenital ZIKV infection in mice proved to be challenging (Zou and Shi, 2017). In the only pioneering study addressing health sequelae in offspring of immunocompetent mice, direct intra-amniotic injection at late gestation (15 days) resulted in motor incoordination and visual dysfunction in survived offspring (Cui et al., 2017). Exposure of immune-compromised (Miner et al., 2016) and immunocompetent mice (Xavier-Neto et al., 2017) to ZIKV at early and mid gestation (5–9 days) results in rapid fetal death and resorption, limiting studies in offspring. Also, in two previous ZIKV reports, rodents have repeatedly cannibalized their morbid offspring shortly after birth, which extremely complicates ZIKV sequelae studies (Li et al., 2016; Siddharthan et al., 2017). NHP apparently provide most relevant data, but NHP are expensive (Morrison and Diamond, 2017), and only two published studies report experimental ZIKV infection in several NHP fetuses before birth (Adams Waldorf et al., 2016; Nguyen et al., 2017). Outcomes of *in utero* ZIKV infection in offspring of NHP are not known. Therefore, the identification of another mammalian species able to at least partially model ZIKV infections in humans has significant value.

In addition to mice and NHP, pigs are also considered as a useful model for preclinical studies (Lind et al., 2007; Vodička et al., 2005). Domestic pigs are closely related to humans regarding anatomy, physiology, genetics, and immunity, and are a relevant animal model to study various human viral infections (Bassols et al., 2014; Gerdts et al., 2015; Meurens et al., 2012) including flavivirus infections (Cassetti et al., 2010; Ilkal et al., 1994; Ricklin et al., 2016). The porcine immune system closely resembles the human immune system (Mair et al., 2014). Progress in swine genomics (Amaral et al., 2009; Prather et al., 2008; Ramos et al., 2009; Tuggle et al., 2007) and biotechnology, including CRISPR technology (Whitworth et al., 2016), have made the development of transgenic pigs just as feasible as the development of transgenic mice (Aigner et al., 2010), conferring an appropriate experimental platform for neurobehavioral and infectious disorders (Alisky, 2006; Baxa et al., 2013; Kragh et al., 2009; Whitworth et al., 2016). A recent increase in the use of pigs as models in neuroscience, cognition, and neurobehavioral studies is due to the close similarity in brain development, growth and anatomy to humans (Dickerson and Dobbing, 1966; Gieling et al., 2011; Glauser, 1966; Lind et al., 2007; Lunney, 2007; Thibault and Margulies, 1998). Porcine models for translational research of schizophrenia (Lind et al., 2005; Lind et al., 2004), antipsychotic interventions (van der Staay et al., 2009), epilepsy (Marchi et al., 2007), intrauterine growth restriction (Bauer et al., 2007; Burke et al., 2006; Ferenc et al., 2014; Gonzalez-Bulnes et al., 2016), learning (Andersen et al., 2016), and social interactions (Kanitz et al., 2016) have been also developed. Pigs are multiparous animals with the same or larger litters than in mice and the length of gestation in pigs, 114 days, closely approximates gestation in humans. Pigs are non-endangered, commercially important agricultural animals, so their use in research is associated with acceptable economic expenses and ethical considerations (Meurens et al., 2012).

From our experience with natural pig infections (Karniychuk and Nauwynck, 2013), at least 10 days of viremia is required for the virus to pass through the placenta. As we previously demonstrated that ZIKV infection in neonatal pigs causes viremia for 5 days (Darbellay et al., 2017), which likely would not be sufficient to induce maternal-fetal transmission in pregnant adult pigs, we chose to inoculate selected porcine conceptuses (a conceptus is a fetus with fetal membranes). Intrauterine and intra-amniotic inoculation in different animal species has also been used in ZIKV (Li et al., 2016; Vermillion et al., 2017), rubella (Amstey, 1969), cytomegalovirus (Chen et al., 2011; Juanjuan et al., 2011), influenza (Collie et al., 1982), simian immunodeficiency virus and human immunodeficiency virus 1 research (Ochs et al., 1993) and have delivered useful information. We did inoculations at 50 gestation days (gd), which corresponds to mid gestation. Twenty-eight days later, we characterized infection in inoculated and non-manipulated conceptuses. We also observed *in utero* affected piglets for 21 days after birth.

2. Materials and Methods

2.1. Virus

We used low-passage, contemporary, Asian-lineage ZIKV strain PRVABC59 (GenBank: KU501215) isolated from human serum collected in Puerto Rico in December 2015. The virus was provided by Centers for Disease Control and Prevention, Division of Vector-Borne Diseases, Fort Collins, Colorado, USA. After two passages on Vero E6 cells, media was centrifuged at 12,000g for 20 min, and supernatants were collected. Media from virus-negative Vero E6 cells was used for mock-inoculation. All inoculums were negative for mycoplasma by PCR (polymerase chain reaction) (Ishikawa et al., 2006).

2.2. Animal Studies

We obtained approval for animal experiments from the University of Saskatchewan's Animal Research Ethics Board and adhered to the Canadian Council on Animal Care guidelines for humane animal use. Pregnant Landrace-cross gilts were housed at the Vaccine and Infectious Disease Organization-International Vaccine Centre (VIDO-InterVac) facilities. Animals were obtained from a high health status herd operated by a recognized commercial supplier.

In utero inoculation was performed at 50 gd (the total duration of porcine pregnancy is 114–115 days) as previously described (Saha et al., 2014; Saha et al., 2010) with some modifications. To establish trans-fetal infection, we manipulated only four conceptuses per gilt (a gilt is a pig pregnant for the first time) (Fig. S1). Three conceptuses (close to the left uterine tip, colored in red in Fig. S1) from three gilts (G296 IP + IA, G313 IP + IA, and G321 IP + IA) were inoculated intraperitoneally + intra-amniotic (IP + IA) with 5 log₁₀ TCID₅₀ (50% tissue culture infective dose) (in 100 μl + 100 μl) of ZIKV. This method of inoculation has been previously used to induce infection (not ZIKV) in porcine fetuses (Saha et al., 2014; Saha et al., 2010). Three conceptuses from other three gilts (G295 IC, G314 IC, and G320 IC) were inoculated intracerebrally (IC) with 4 log₁₀ TCID₅₀ (in 25 μl) of ZIKV. This method of inoculation has been previously used to induce ZIKV infection in mice (Li et al., 2016). For convenience, two different experimental groups along the manuscript are designated as IP + IA and IC. As a manipulation control, one fetus in each litter was mock-inoculated with media from virus-negative cell culture (close to the last or first virus-inoculated fetus; colored in green in Fig. S1). As a surgery control, conceptuses from three control gilts were also mock-inoculated (gilts G270 C, G312 C, and G319 C), two fetuses IC and two fetuses IP + IA in each control gilt. We applied nonabsorbable sutures to the uterine wall adjacent to the inoculated fetuses (in gilts G295 IC, G314 IC, G296 IP + IA, G313 IP + IA, G270 C, and G312 C) to identify fetuses after gilt euthanasia. Gilts G295 IC, G314 IC, G296 IP + IA, G313 IP + IA, G270 C, and G312 C were euthanized and sampled 28 days post *in utero* inoculation (Fig. S1). Uteri with fetuses were removed. Amniotic fluid (AF), amniotic membranes (AM) and uterine wall with the placenta (PL) (fetal placental compartment was subsequently dissected from the maternal endometrium) were collected from each conceptus and rapidly frozen. Amniotic fluids were aspirated with sterile syringes with needles before tissue dissection. All samplings were performed in direction from a non-manipulated conceptus closest to the right uterine horn tip toward inoculated fetuses (Fig. S1). Fetuses were visually examined. Body length and head diameter (from ear to ear with a digital caliper) in fetuses (from litters G312 C, G314 IC, and G313 IP + IA) were measured with a tape and electronic caliper, respectively. The gender of fetuses was recorded as well. Blood plasma and brain were collected from all fetuses. Prior to tissue collection, fetuses from gilts G312 C (7 fetuses), G314 IC (14 fetuses), and G313 IP + IA (9 fetuses) were scanned with computed tomography (CT) and chosen fetuses (9 fetuses, 3 from each gilt) with magnetic resonance imaging (MRI). In these litters, to reduce manipulation time and obtain quality imaging and tissue samples, AM and PL

were not sampled. Maternal plasma, uterine lymph nodes (LN) and endometrium were collected from gilts.

Blood samples from gilts G319 C, 320 IC and G321 IP + IA were sampled during gestation (50 and 78 gd) and after parturition (at days 0 and 21). Milk was also sampled at 7 days after parturition. After euthanasia (21 days after parturition) maternal uterine LN and endometrium were sampled and frozen. We monitored births closely, and randomly collected rejected after birth placental tissues and amniotic membranes. We collected blood from piglets at 0, 7, 14, and 21 days post birth. Body length and weight in neonates were recorded at 1 and 21 days post birth. We monitored piglets every day. Shortly after birth, and then weekly, the same person was observed animals for at least 1 h, and videos were recorded. After euthanasia (21 days post birth), piglet brains were weighed and sampled. The left brain hemisphere was frozen in liquid nitrogen. The right hemisphere was preserved in formalin.

Blood plasma from all fetuses and gilts, tissues from dead fetuses, and plasma from neonates were screened with previously validated polymerase chain reaction (PCR) assays to exclude common porcine fetal pathogens - porcine reproductive and respiratory syndrome virus (PRRSV) (Mardassi et al., 1994), porcine parvovirus (PPV) (Wilhelm et al., 2006), porcine circovirus 1 (PCV1), and porcine circovirus 2 (PCV2) (Larochelle et al., 1999). All samples were negative.

2.3. Reverse Transcription Polymerase Chain Reaction (RT-PCR)

RNA (ribonucleic acid) from AF and blood plasma was extracted using QIAamp Viral RNA Mini Kit (QIAGEN, USA). Tissues were weighed and homogenized in 600 μ l RLT buffer (placenta, amniotic membranes, maternal LN and endometrium) or 1 ml QIAzol Lysis Reagent (fetal cerebrum and cerebellum) using RNase-free stainless steel beads and TissueLyser II (QIAGEN, USA) operating for 5 min at 25 Hz. RNA was extracted using the QIAGEN RNeasy Mini extraction kit (placenta, amniotic membranes, maternal LN, and endometrium) or QIAGEN RNeasy Lipid Tissue Mini Kit (fetal cerebrum or cerebellum). A previously published ZIKV specific real-time RT-PCR SYBR Green assay was used for ZIKV RNA quantification (Xu et al., 2016). As a positive PCR control, we used Vero E6 cell culture media containing ZIKV. As a negative control, we used samples from mock-inoculated and non-manipulated control fetuses. Strict precautions were taken to prevent PCR contamination. Aerosol-resistant pipette tips and disposable gloves were always used. Reagent controls, with water instead of body fluid or tissue samples, were included in every RNA isolation and PCR run. All PCR reactions were conducted with SensiFAST SYBR Lo-Rox One-Step Kit reagents (Bioline, USA) on the StepOne Plus platform (Life Technologies, USA) and analyzed using StepOne software version 2.3. Relative viral loads were determined using RNA from a stock of ZIKV with a known infectious TCID₅₀ titer to generate a PCR standard curve. Relative log₁₀ TCID₅₀ values were defined as RNA units (U) and expressed as ZIKV RNA U per ml of AF or plasma. Relative values from tissue samples were corrected for their weight and expressed as ZIKV RNA U per g.

2.4. Virus Titration on Vero E6 Cells

Tissue homogenates and body fluids were serially diluted twofold in four replicates starting at a dilution of 1:2, and 50 μ l of each dilution was added to confluent Vero E6 cells cultured in 96-well plates in DMEM media (Thermo Fisher Scientific, USA) supplemented with 10% fetal bovine serum (FBS) (Sigma-Aldrich, USA). After 2 h of incubation, the inoculum was removed, and fresh media (2% FBS) was added. The cells were incubated for 5 days before plate washing and drying. The plates were kept at -20°C at least for 2 h or until use. Plates were thawed and then fixed in 10% buffered formalin (Fisher Chemical, USA) for 20 min, washed twice with PBS and incubated with methanol with 0.3% H₂O₂ (Sigma-Aldrich, USA) for 10 min. Plates were washed twice with PBS (phosphate buffered saline) and 50 μ l of affinity-purified rabbit anti-ZIKV polyclonal antibodies (Ab) (1.3 μ g/ml working dilution;

IBT BIOSERVICES, USA; peptide sequence to ZIKV E glycoprotein was used as immunogen to produce Ab; Ab are verified in Western blot and ELISA (enzyme-linked immunosorbent assays) by a manufacturer) with 10% goat serum (Thermo Fisher Scientific, USA) were added per well, followed by incubation at 37 $^{\circ}\text{C}$ for 1 h. Plates were washed three times with PBS containing 0.05% Tween 80 and 50 μ l of goat anti-rabbit IgG conjugated with horseradish peroxidase (HRP) (1/2000 working dilution; Abcam, USA) with 10% goat serum were added per well, followed by incubation at 37 $^{\circ}\text{C}$ for 1 h. Plates were washed three times, and 50 μ l of aminoethyl carbazole (AEC) (Sigma-Aldrich, USA) solution in acetate buffer was added to each well, after which plates were incubated at room temperature for 25 min. Then the reaction was stopped by replacing the substrate with an acetate buffer and ZIKV-specific staining was determined by examination with a microscope. ZIKV titers were determined using the Reed and Muench method (Reed and Muench, 1938). As a positive control, we used Vero E6 cell culture media containing ZIKV. Body fluid and tissue samples from mock-inoculated and non-manipulated control piglets were used as negative controls.

2.5. Serological Responses

For quantification of ZIKV-specific IgM and IgG Ab modified immunoperoxidase monolayer assay (IPMA) (Wensvoort et al., 1991) was used as previously described (Darbellay et al., 2017). Vero E6 cells in 96-well cell culture plates were inoculated with 50 μ l media containing 2.3 log₁₀ TCID₅₀ per ml ZIKV and incubated for 72 h (37 $^{\circ}\text{C}$, 5% CO₂). Then the culture medium was removed and plates were washed and dried. The plates were kept at -20°C until use. Plates were thawed and then fixed in 10% buffered formalin for 20 min. Cells were washed twice with PBS and incubated with methanol with 0.3% H₂O₂ for 10 min. Plates were washed twice with PBS and two-fold serial dilutions of heat-inactivated plasma or milk (56 $^{\circ}\text{C}$ for 30 min) were added (first dilution is 1:2 for fetal samples; for neonatal and maternal samples 1:10), followed by incubation for 1 h at 37 $^{\circ}\text{C}$. Plates were washed three times with PBS containing 0.05% Tween 80 and after addition of 50 μ l of goat anti-swine IgM (1/40 working dilution; KPL, USA) or rabbit anti-pig IgG (1/500 working dilution; Abcam, USA) Ab conjugated with HRP per well, plates were incubated at 37 $^{\circ}\text{C}$ for 1 h. Afterward, plates were washed and AEC solution was added. Specific staining was determined as described above. Plasma and milk from mock-inoculated and non-manipulated control fetuses and gilts were used as negative controls.

We quantified ZIKV neutralizing Ab (NAb) with neutralizing assay as described before (Darbellay et al., 2017; Lefebvre et al., 2008) with some modifications. Fifty μ l of ZIKV (2 log₁₀ TCID₅₀/ml) were mixed with equal volumes of heat-inactivated, two-fold serially diluted plasma or milk (for fetal samples first dilution is 1:4; for piglet and maternal samples 1:10; in two replicates) and incubated at 37 $^{\circ}\text{C}$ for 1 h, before inoculation onto Vero E6 cells in 96-well plates. After 2 h fresh media was added. After 120 h cells were fixed and stained with ZIKV-specific Ab as described for virus titration. The NAb titers were defined as the reciprocal of the highest serum dilution that inhibited ZIKV infection in 50% of the inoculated wells. Sera from mock-inoculated and non-manipulated control fetuses and gilts were used as negative controls.

2.6. Bio-Plex Assay

Bio-Plex assay reagents are listed in Table S1. We measured interferon alpha (INF α), interleukin-8 (IL-8), interleukin-10 (IL-10), interferon gamma (INF γ), interleukin-1b (IL-1b), interleukin-6 (IL-6), interleukin-12 (IL-12), interleukin-13 (IL-13), interleukin-17A (IL-17A) in amniotic fluids and blood plasma as previously described (Pasternak et al., 2014) with some modifications. Briefly, Bio-Plex bead coupling was performed as per the manufacturer's instructions. The multiplex assay was carried out in a 96 well Greiner Bio-One Fluotrac 200 96F black plates (VWR, USA). The beadsets conjugated with the capture

antibodies were vortexed for 30 s followed by sonication for another 30 s to ensure total bead dispersal. The bead density was 1200 beads/ μl in PBS-BN (1 \times PBS pH 7.4 + 1% bovine serum albumin (Sigma-Aldrich, USA) + 0.05% sodium azide (Sigma-Aldrich, USA)). 1 μl of each beadset was added to diluent (PBS + 1% porcine serum + 0.05% sodium azide) for a total volume of 50 μl per well. The plate was then washed using the Bio-Plex Pro II Wash Station (BioRad, USA; wash 2 \times 100 μl PBST (phosphate buffered saline with Tween 20)). The protein standards with starting concentrations as indicated in the table were mixed together in diluent and 2.5 fold dilutions done to produce the standard curve. 50 μl per well of each dilution was added to the plate. Sera were prediluted 1:4, amniotic fluid diluted 1:2 and added to the wells at 50 μl per well in duplicate. The plate was agitated at 800 rpm for 1 h at room temperature. After 1 h incubation with the samples, the plate was washed (3 \times 150 μl PBST). 50 μl of a biotin cocktail (consisting of the biotins diluted as indicated in Table S1) was added to each well. The plate was again sealed, covered and agitated at 800 rpm for 30 min at room temperature then washed again as indicated above. 50 μl of Streptavidin RPE (Prozyme, USA; diluted to 5 $\mu\text{g}/\text{ml}$) was added to each well. The plate was again sealed, covered and agitated at 800 rpm for 30 min at room temperature and washed as indicated above. A 100 μl of 1 \times Tris-EDTA was added to each well and then the plate was vortexed for 5 min before reading on the BioRad Bio-Plex 200 instrument following the manufacturer's instructions. The instrument was set up to read beadsets in appropriate regions. A minimum of 60 events per beadset were read and the median value obtained for each reaction event per beadset. For all samples the multiplex assay data was corrected by subtracting the background levels.

2.7. Computed Tomography and Magnetic Resonance Imaging

Fetal head CT scanning was performed using a Toshiba CT unit (16 slices) without contrast, and MRI was performed using a Siemens 1.5 Tesla MRI scanner. The MRI sequences used for analysis were T1, T2 and PD weighted images. CT scans were performed with 1 mm slice equivalence, 200 mA and 80 kVp. We reviewed the CT scans for ventricular dilation and evidence of abnormal mineralization. MRI scans were reviewed for abnormal mineralization, cerebral ventricular enlargement, subjective assessment of brain volume, abnormalities of the cisterna magna and corpus callosum. We considered mainly T2 weighted images as the most useful sequence.

2.8. Histology

Formalin-fixed brain tissues from fetuses were embedded in paraffin, sectioned and stained with hematoxylin and eosin (H&E). The entire tissue sections were scanned using Aperio Scanscope CS (Leica Biosystems, USA) at a magnification of $\times 20$, and scans were examined and analyzed using Image-Scope-Rev.-v12.1.0.5029 software for calcifications, white and grey matter ratio and lesions. Formalin-fixed brain tissues from piglets were embedded in paraffin, sectioned and stained with H&E. Sequential tissue sections were examined under a microscope. Only frozen fetal membranes were available for analyses. Frozen uterus with placenta tissues collected from conceptuses at 28 days post inoculation and placental tissues rejected during the birth were sectioned on a cryostat. After H&E staining, sequential sections were examined under a microscope. The quality of tissue presentation of frozen placental samples, however, was not suitable for histological evaluation.

2.9. In situ Hybridization

RNA *in situ* hybridization (ISH) was performed with RNAscope 2.5 HD Reagent Kit-BROWN (Advanced Cell Diagnostics, USA) according to the manufacturer's instructions for frozen tissues. The RNAscope V-ZIKV probe targeting ZIKV RNA (catalog no. 467771), positive control Sc-PPIB probe targeting pig PPIB gene (catalog no. 428591), and

RNAscope negative control DapB probe (catalog no. 310043) probes were designed and synthesized by Advanced Cell Diagnostics. Tissues were counterstained with hematoxylin and visualized with standard bright-field microscopy. To monitor the specificity of the staining, tissues from mock-exposed and ZIKV-exposed fetuses were treated with ZIKV-specific and negative control probes, respectively.

2.10. RNA-Seq and Bioinformatics

RNA was isolated using TRIzol (Thermo Fisher Scientific, USA) lysis and extraction, and then cleaned using Total RNA Purification Kit (Norgen Biotek, Canada). RNA was assessed on a bioanalyzer and all samples had RNA Integrity Number values above 8.5. cDNA (complementary DNA) sequencing libraries were prepared using Illumina RIBO Gold Kit and TruSeq Stranded Total RNA Library Prep Kit (Illumine, USA). Libraries were sequenced on a NextSeq500 as paired end reads using the 75 base kit. Approximately 30 million paired end reads per sample were generated. FASTQ files were trimmed for adaptor sequences and filtered for low quality reads using *cutadapt*. Trimming was visually checked using FastQC. Paired end reads were aligned using *bowtie* as local alignments to cDNA sequences representing coding and non-coding transcripts taken from ENSEMBL *Sus scrofa* build 10.2. Mapped reads were sorted and the header information for each alignment separated into a text file. The file was then turned into a counts table using custom shell and R scripts. The counts table was then analyzed by *DESeq2* to generate normalized data and *voom* for differential expression.

A weighted ranked list was generated by multiplying the \log_2 fold change with the $-\log_{10}$ for the p-value. The product of the p-value gives more weight to those fold changes with some degree of statistical significance. The fold change keeps the direction of the change either positive or negative. These were used in the GSEA (Gene Set Enrichment Analysis) of preranked list function and tested against the GO (Gene Ontology) biological processes.

The GSEA results for both IC and IP + IA treatment groups were graphed in *Cytoscape* using the EnrichmentMap plugin. Both groups were plotted against each other with G296 IP + IA as data set 1 and G295 IC as dataset 2. A network was generated using a Jaccard + Overlap with a cutoff of 0.375 and a Combined Constant of 0.5. Sub-networks were annotated using the WordCloud plugin and words were scaled to 0.3 *versus* the network to rank both unique words *versus* the network and high frequency words within the sub-network. The top 4 words were used to annotate the subnetworks.

Gene Expression Omnibus accession number for RNA-seq data is GSE103932.

2.11. Data Analysis

We used GraphPad PRISM™ 7 software (GraphPad Software Inc., San Diego, CA, USA) for statistical analyses. The normally distributed data were analyzed with Fisher exact test or one-way ANOVA following by a pairwise comparison with Tukey's test. The data which did not distribute normally were analyzed with Mann-Whitney rank sum test or ANOVA on Ranks following by a pairwise comparison with Dunn's test. The difference in the number of mummified fetuses between infected and control litters was analyzed with the Chi-square test. Pearson Product-Moment Correlation coefficient was applied to analyze linear correlation. Linear regression was applied to model kinetics of *in utero* ZIKV infection. A p-value < 0.05 was considered statistically significant. Graphs were prepared in R ggplot2.

3. Results

3.1. ZIKV Causes Persistent Infection in Porcine Conceptuses

We directly inoculated selected conceptuses *in utero* with ZIKV either intracerebrally (IC) (G295 IC, G314 IC, and G320 IC gilts) or

intraperitoneally + intra-amniotic (IP + IA) (G296 IP + IA, G313 IP + IA, and G321 IP + IA gilts) at 50 gd (Fig. S1). Litters with mock-inoculated conceptuses from three gilts (G270 C, G312 C, and 319C gilts) were used as controls. Conceptuses from gilts G295 IC, G314 IC, G296 IP + IA, G313 IP + IA, G270 C, and G312 C were sampled 28 days after inoculation. Gilts G320 IC, G321 IP + IA, and G319 C delivered piglets at term, and we observed piglets for 21 days after birth.

We sampled 24 and 62 conceptuses from two control (G270 C and G312 C, not shown) and four experimental (G295 IC, 314 IC, G296 IP + IA, and G313 IP + IA) gilts (Fig. S1). Control and experimental litters contained one (4%) and seven (11%) mummified fetuses, which were not statistically different ($p = 0.64$ Chi-square test; $p = 0.29$ Fisher exact test) and are in line with rates of fetal mortality in pigs of 7.5% (Vanderhaeghe et al., 2010) to 30% (Tayade et al., 2006). The mummification process prevented extraction of RNA suitable for PCR detection of ZIKV. Cranium and body measurements of viable fetuses were not significantly different between litters (body length, $p = 0.08$; cranium diameter, $p = 0.3$; ANOVA on ranks) (Table S2).

As in a previous human study (Bhatnagar et al., 2017; Tabata et al., 2016), we detected ZIKV RNA in fetal membranes. ZIKV was detected in samples from directly inoculated and non-manipulated adjacent and distant siblings (Fig. 1). Viral titers in the PL and AM ranged from 1.0 to 5.6 ZIKV RNA U per g (mean 3.2 ± 1.3) and from 1.1 to 6.4 ZIKV RNA U per g (mean 4.2 ± 1.7) (Fig. 1a). Like in human fetuses, pig conceptuses also contained high viral titers in AF, ranging from <0.1 to 5.1 ZIKV RNA U per ml (mean 2.8 ± 2.0) (Fig. 1a). We were not able to isolate infectious virus from PL and AM tissues on Vero E6 cells. High infectious ZIKV titers, however, were detected in AF from directly inoculated and trans-infected conceptuses (range from <1.2 to 4.0 ZIKV log₁₀ TCID₅₀ per ml (mean 0.6 ± 1.0) (Fig. 1b), reflecting productive, persistent infection in conceptuses for at least 28 days. We also detected

ZIKV RNA by ISH in fetal placental mesenchyme and AM (Fig. 2a, Fig. 2b) suggesting persistent infection in fetal membranes. Maternal blood, endometrium, and maternal uterine lymph nodes (LN) were free from ZIKV RNA and infectious virus. Fetal samples from control litters were negative for ZIKV.

In humans and mice, it has been demonstrated that the type I interferons are essential to the host defense mechanisms against ZIKV (Hamel et al., 2015; Lazear et al., 2016; Vermillion et al., 2017). At 28 dpi, we found elevated INF α levels in AF and plasma of directly inoculated and non-manipulated porcine conceptuses, which suggests productive ZIKV infection (Fig. 3a). Levels of INF α were below the detection limit in all control conceptuses (Fig. 3a). Levels of INF α in AF and plasma of IP + IA litters were significantly higher than in control (C) and IC litters. The difference between C and IC litters was not significant, but a trend to increase of INF α in IC litters was evident (Fig. 3a). Levels of INF α in AF of IP + IA litters strongly correlated with ZIKV PCR titers in AF ($r = 0.714$, $p = 0.00009$; Pearson correlation test). The trend to positive correlation was also observed in IC litters ($r = 0.348$, $p = 0.06$; Pearson correlation test). IP + IA litters also had significantly higher levels of IL-8 in AF (Fig. 3b). All litters had similar concentrations of IL-10 in AF and plasma (Fig. 3c). Levels of INF γ , IL-1b, IL-6, IL-12, IL-13, and IL-17A were below the detection limits.

ZIKV RNA loads in PL, AM, and AF of non-manipulated fetuses from IC litters and in AF from IP + IA litters negatively correlated with the distance to the nearest directly inoculated sibling (Fig. S2). The regression analysis also suggests that ZIKV passes faster from fetus to fetus in the IP + IA litters than in the IC litters. As such, ZIKV RNA was distributed more evenly in PL and AM of non-manipulated fetuses in the IP + IA litter than in the IC litter (Fig. S2). Also, PCR and infectious ZIKV titers in PL and AF were significantly higher in IP + IA litters than in IC litters (Fig. 1a, $p = 0.038$ for PL, $p = 0.008$ for AF; Fig. 1b, $p = 0.001$ for AF; by the Mann-Whitney rank sum test).

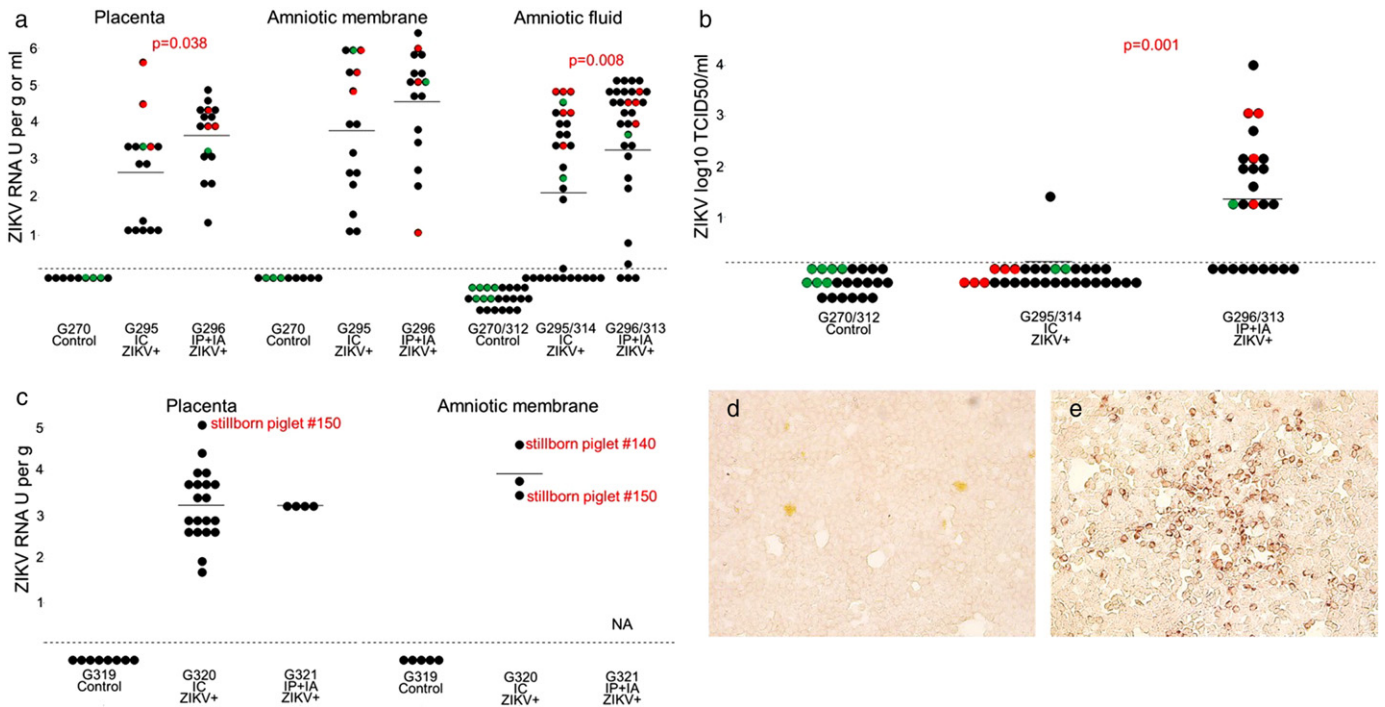


Fig. 1. ZIKV in fetal membranes and amniotic fluids. (a) ZIKV PCR titers in the placenta, amniotic membranes and amniotic fluid of fetuses from virus-exposed litters. Dots represent results in each sample collected from fetuses. Relative log₁₀ TCID₅₀ values were defined as RNA units (U) and expressed as ZIKV RNA U per gram (g) of tissues or milliliter (ml) of fluids. A dotted line represents the assay detection limit. Dots below the detection limit are negative samples. Green dots represent fetuses mock-challenged intracerebrally (IC) or intraperitoneally + intra-amniotic (IP + IA). Red dots represent fetuses directly challenged with ZIKV IC or IP + IA. Black dots represent non-manipulated fetuses. X-axis represents gilt identification and method of litter exposure. We used Mann-Whitney rank sum test to compare ZIKV titers in the placenta and amniotic membranes collected after birth from the G320 IC and G321 IP + IA litters. (b) Infectious ZIKV TCID₅₀ titers in amniotic fluids of fetuses from virus-exposed litters. (c) ZIKV loads in the placenta and amniotic membranes collected after birth from the G320 IC and G321 IP + IA litters. ZIKV-specific immunohistochemistry staining in Vero E6 cells inoculated with amniotic fluid from control (d) and ZIKV-positive (e) fetuses. Brown staining represents active viral replication in cells.

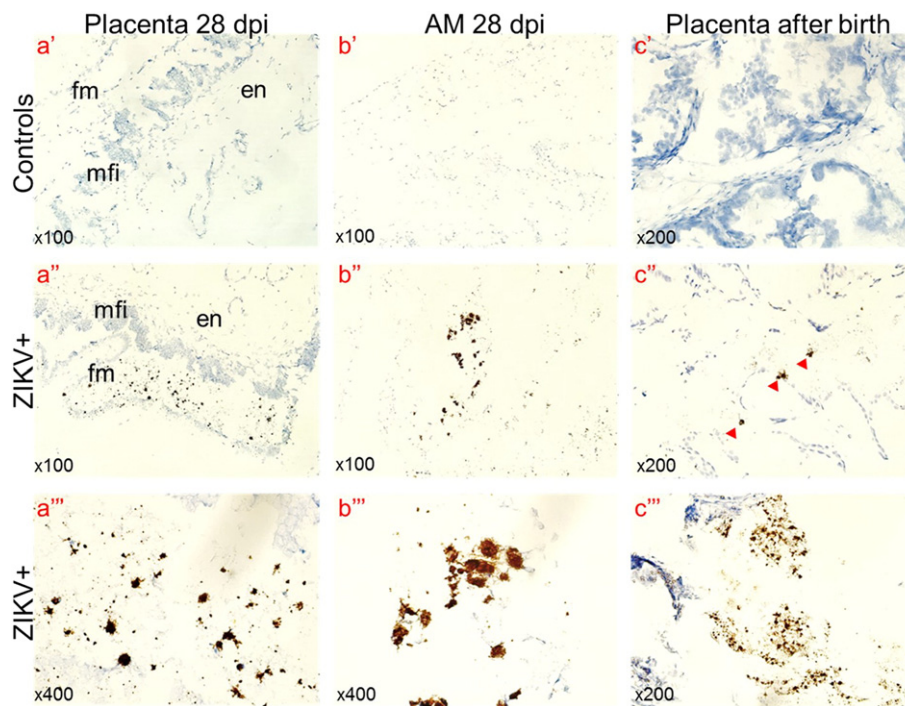


Fig. 2. ZIKV-specific ISH in the placenta and amniotic membranes. Brown staining indicates ZIKV RNA. Control samples from mock-exposed fetuses and tissues from ZIKV-exposed fetuses treated with ZIKV-specific and negative control probe, respectively, had no staining. AM – amniotic membrane; dpi – days post inoculation (a) we tested selected placental samples from the G296 IP + IA litter (Fetus #5, 6, 7, 10, 14 and 16), specific staining was observed in fetal placental mesenchyme from fetuses #6 and #16. Amnion from fetus #16 (b) also contained ZIKV-specific staining. fm – fetal placental mesenchyme; en – maternal endometrium; mfi – the maternal-fetal interface consisting of fetal trophoblast and maternal uterine epithelium. (c) We tested selected placental tissues rejected after the birth of G320 IC (seven samples) and G321 IP + IA (four samples) litters. One sample (14%) in the G320 IC litter and three samples in the G321 IP + IA litter (75%) contained ZIKV-specific staining. Staining was more intensive in samples from the G321 IP + IA litter (c'') than in the G320 IC litter (c'). Red arrowheads indicate regions with ZIKV positive cells.

ZIKV RNA was detected at similar low rates ($p = 0.482$, by the Mann-Whitney rank sum test) in fetal blood plasma from both IC litters (27%, 8 fetuses; mean = 0.119 ± 0.32 RNA U/ml) and IP + IA (36%, 9 fetuses; mean = 0.129 ± 0.259 RNA U/ml) (Fig. S1).

All PL and AM samples from the G320 IC and G321 IP + IA litters collected after birth, including available samples from stillborn fetuses, had high ZIKV titers (Fig. 1c). Yet we did not isolate infectious virus on Vero E6 cells from PL and AM. Other groups have also reported difficulties in isolating infectious ZIKV from human fetal tissues with pathology (Mlakar et al., 2016; Moura da Silva et al., 2016) and from tissues of immunocompetent animals (Adams Waldorf et al., 2016). However, we detected ZIKV RNA by ISH in after birth placental samples by ISH (Fig. 2c), suggesting persistent infection in conceptuses for one-two months (from inoculation at 50 gd to birth 114 gd). In accordance to distinct *in utero* infection kinetics (Fig. S2) and intensity (Fig. 1) in IP + IA and IC litters, the percentage of ZIKV-positive samples and intensity of ISH staining was higher in samples from the G321 IP + IA litter than in samples from the G320 IC litter (Fig. 2c). Maternal plasma, endometrium and uterine LN, and neonatal plasma from the control G319 C litter were negative for ZIKV.

3.2. ZIKV Causes Infection and Molecular Pathology in the Porcine Fetal Brain

ZIKV RNA was detected by PCR (Fig. 4a) and by ISH (Fig. 4b), in the cerebral and cerebellar cortex from inoculated and non-manipulated IC and IP + IA fetuses. Significantly, the same tissue tropism is described in humans, NHP, and mice (Bhatnagar et al., 2017; Mlakar et al., 2016; Osuna et al., 2016). Brain samples from control fetuses were negative for ZIKV. At this stage of infection and fetal development, no histological differences were observed between control and infected litters (Fig. S3). Computed tomography and MRI also did not show significant differences between infected and non-infected fetuses (Fig. S3; Dataset S1).

We did not identify ZIKV RNA in blood plasma and brains from offspring. Offspring also did not have brain lesions or histopathology (Fig. S3).

Because we found ZIKV in fetal brain samples, we sought to characterize molecular pathology in the developing brain. We dissected fetal cerebrum tissues for RNA-seq in line with our data (Fig. 4b) and previous findings that suggested ZIKV primarily localized to the cerebrum (Mlakar et al., 2016; Retallack et al., 2016). To avoid effects of the vehicle and manipulation on gene expression, we selected ZIKV-positive brain samples from non-manipulated, trans-infected fetuses (Table S3). As we found the different intensity of infection in IC and IP + IA litters (Fig. S2), we treated RNA-seq data as IC or IA + IP groups. Indeed, while principal component analysis (PCA) showed a good grouping of control samples, the samples from infected cerebrums were largely separated by the group (Fig. S4). The sequences from the IC group clustered at a small but distinct distance from controls. In contrast, fetuses from the IP + IA group showed a greater, but less uniform separation from controls, suggesting that a more prolonged ZIKV infection in fetal membranes or brain has more significant effect on gene expression in the cerebrum. One of the three fetuses from the IP + IA group clustered in with the IC group (Fig. S4). This fetus in the IP + IA group was the only one with Ab against ZIKV (Table S3), indicating a distinct immunological status. Therefore, we removed this fetus from the RNA-seq data analysis. But, it is worthwhile to note that fetuses may be able to mount immune responses that might be protective from infection-induced molecular pathology. Using the *voom* function in *limma* (Bioconductor) we calculated the differential gene expression between IC, IP + IA, and control groups. As there were only two samples from the IP + IA group, we used the fold change calls and the p-value to generate a weighted ranked list. We tested data from IC and IP + IA groups in GSEA with the GO biological process GMT file, plotting of the data in Cytoscape using the enrichment map plugin for terms with a < 0.025 p-value to generate multiple sub-networks (Fig. 4c). Interestingly, the

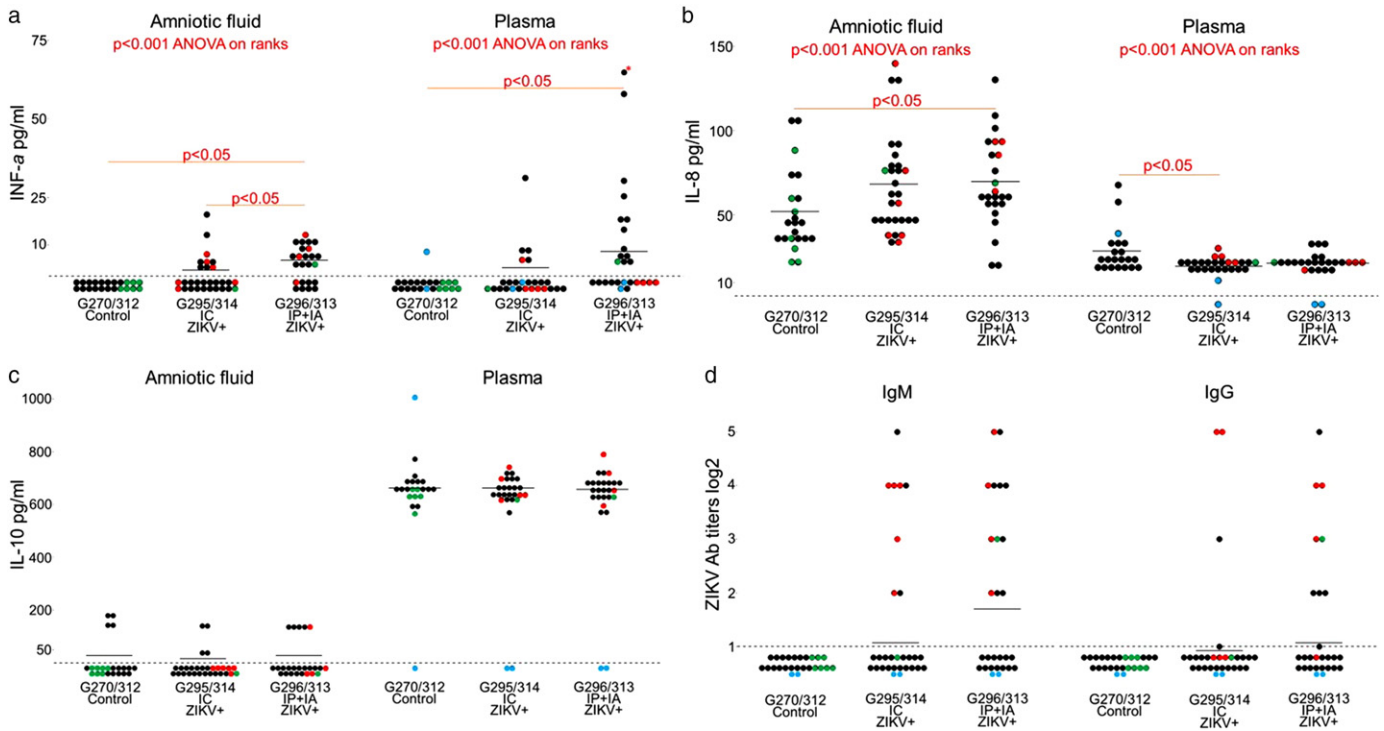


Fig. 3. Cytokine concentrations and ZIKV-specific Ab responses in fetuses. (a–c) INF α , IL-8, and IL-10 concentrations in amniotic fluid and fetal blood plasma. G270 C and 312C – control litters; G295 IC and 314 IC – selected fetuses in these litters were intracerebrally inoculated *in utero* with ZIKV; G296 IP + IA and 313 IP + IA – selected fetuses in these litters were intraperitoneal + intra-amniotic inoculated *in utero* with ZIKV. A dotted line represents the assay detection limit. Dots below the detection limit are negative samples. Green dots represent fetuses directly mock-inoculated IC or IP + IA. Red dots represent fetuses directly inoculated with ZIKV IC or IP + IA. Black dots represent non-manipulated fetuses. Blue dots represent cytokine concentration in maternal blood plasma. Difference between litters was tested with ANOVA on Ranks following by a pairwise comparison with Dunn's test. * - in panel (a) indicates a sample which is above the graph scale; fetus #5, 180.4 pg/ml. (d) Zika virus-specific antibodies in fetuses from IC and IP + IA exposed litters. A dotted line represents the assay detection limit. Dots below the detection limit are negative samples. Green dots represent fetuses directly mock-inoculated IC or IP + IA. Red dots represent fetuses directly inoculated with ZIKV IC or IP + IA. Black dots represent non-manipulated fetuses. Blue dots represent maternal blood plasma.

network graph (Fig. 4c) indicated that ZIKV infection may affect pathways related to interferon production, mitosis, dendritic spine and synapse organization, glial cells, and embryonic brain development (metencephalon and telencephalon). All enriched and depleted GO pathways are listed in Dataset S2-Sheet 5–8. We also tested a set of genes related to Antiviral Responses (Fig. S5) assembled from previous ZIKV publications (Bayer et al., 2016; Hamel et al., 2015; Li et al., 2016; Quicke et al., 2016), and found that infected fetuses from the IP + IA and IC groups were enriched in this term (False discovery rate (FDR) corrected p-value = 0.102 for the IP + IA group and FDR p-value = 0.175 for the IC group, where FDR p-value < 0.25 is considered significant).

To gain insight into the similarities of the porcine model to human disease we generated gene sets compiled from MalaCards (<http://www.malacards.org>) and previous publications (Li et al., 2016; Moura da Silva et al., 2016; van der Linden et al., 2016; Zhang et al., 2016) linked to the following clinical disorders associated with congenital Zika syndrome in human fetuses and neonates: microcephaly (Li et al., 2016), epilepsy (Lemke et al., 2012), dysphagia (Jaradeh, 2006), clubfoot (Hecht et al., 2007; Heck et al., 2005; Shyy et al., 2009), and arthrogryposis (Dohrn et al., 2015; Jonsson et al., 2012) (Table S4). Additionally, we collected gene sets from MalaCards for: Guillain-Barre Syndrome, Schizophrenia, Attention Deficit-Hyperactivity Disorder, Psychotic Disorder, Anxiety Disorder, Mood Disorder, and Learning Disability (Table S4).

Similar to above we tested these custom gene sets using GSEA and found that infected fetuses from the IC group were enriched in Mood Disorder term, and depleted in terms Microcephaly, Epilepsy, and Schizophrenia (FDR p-value = 0.20; Fig. S6, Dataset S2-Sheet 9). Taking a more stringent approach we clustered the 669 differentially expressed

genes (FDR < 0.05; Dataset S2-Sheet 1) between the control and ZIKV exposed fetuses (Fig. 4d). We noted a small up-regulated set of genes that was found in both IP + IA and IC groups (Fig. 4d–e). This small set of genes was significantly enriched in a number of GO pathways related to virus, defense, immune, interferon, and stress responses (Dataset S2-Sheet 4).

3.3. ZIKV-Specific Ab Responses in Porcine Fetuses and Mothers

Like ZIKV-affected human fetuses (Oliveira et al., 2016), porcine fetuses showed ZIKV-specific Abs (Fig. S1; Fig. 3d). Since mothers did not have ZIKV Ab at this time of sampling (Fig. 3d), Ab were of fetal origin. Also, maternal Ab do not pass to porcine fetuses through the placenta (Sterzl et al., 1966). When tested *in vitro*, fetal plasma containing ZIKV Ab could not neutralize infection (neutralizing Ab titers < 1:4). Samples from all gilts and control fetuses were negative for ZIKV-specific Ab at 28 days post inoculation (78 days of gestation).

Plasma from all piglets in both G320 IC and G321 IP + IA litters, except two stillborn piglets from the G320 IC litter (stillborn piglets #140 and #170; interestingly, AM from stillborn pig #140 had high ZIKV titers (Fig. 1c)), contained virus binding IgG and neutralizing Ab (NAb) at birth (114 days of gestation), 7, 14, or 21 days later (Fig. 5a–b). IgM Ab in piglets were below the detection limit. Plasma samples from control piglets were negative for Ab.

A direct challenge of selected conceptuses *in utero* resulted in ZIKV transmission to non-manipulated adjacent and distant siblings, and caused maternal infection as indicated by high titers of ZIKV specific virus binding IgG Ab in maternal plasma and milk at birth and three weeks later (Fig. 5c). We also detected NAb in maternal plasma (Fig. 5d). IgM Ab in plasma and milk from all gilts were below the

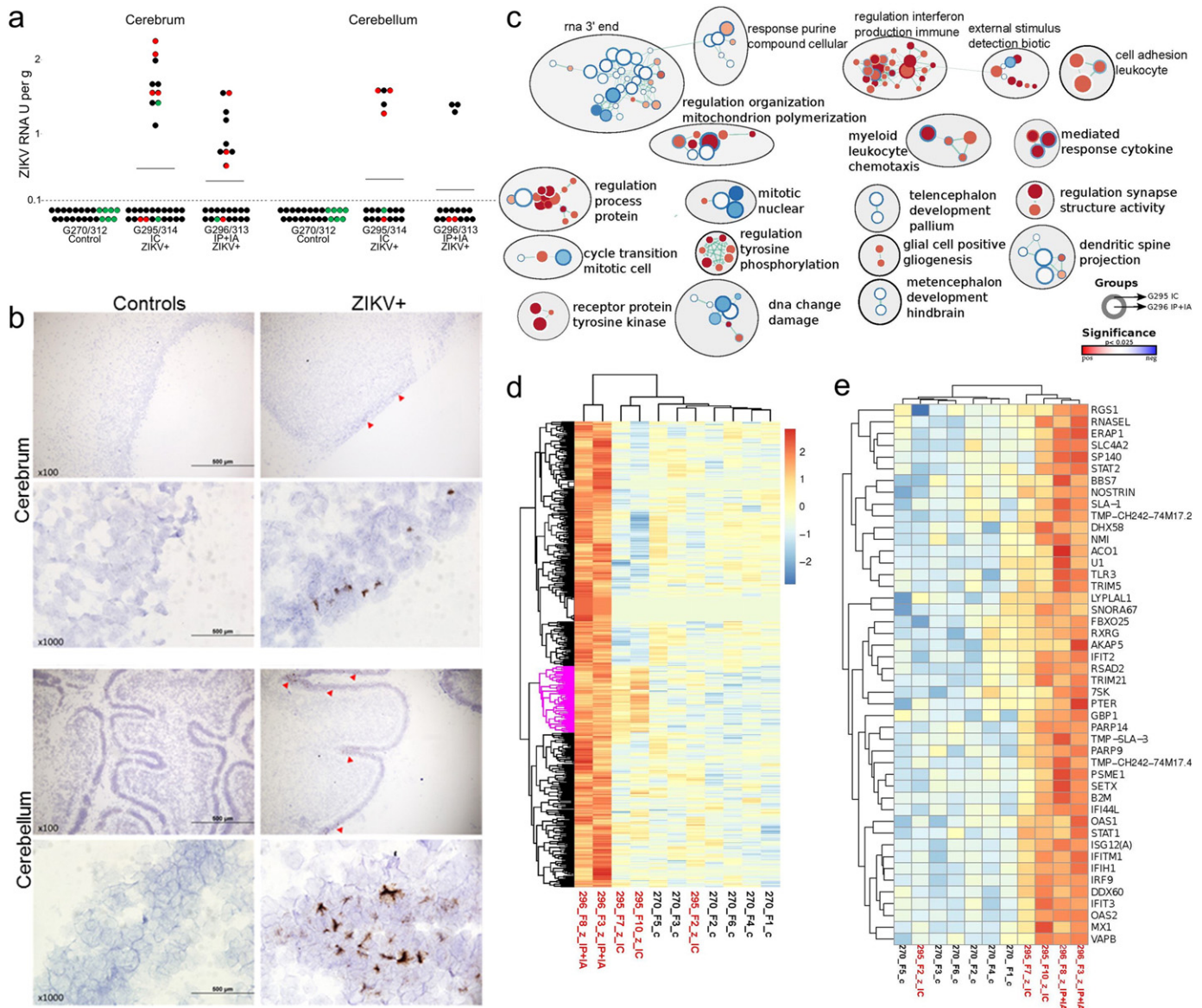


Fig. 4. ZIKV infection and molecular pathology in fetal brains. (a) PCR titers in the cerebrum and cerebellum. A dotted line represents the assay detection limit. Dots below the detection limit are negative samples. Green dots represent fetuses directly mock-inoculated IC or IP + IA. Red dots represent fetuses directly inoculated with ZIKV IC or IP + IA. Black dots represent non-manipulated fetuses. Dots with yellow demarcations represent samples positive for ZIKV RNA by *in situ* hybridization. Two fetuses (9%) out of 23 tested by ISH had virus RNA in the cerebral cortex. Two fetuses (15%) out of 13 tested by ISH had virus RNA in the cerebellar cortex. (b) ZIKV-specific *in situ* hybridization staining in the fetal cerebrum and cerebellum. Brown staining indicates ZIKV RNA. Control samples from mock-exposed fetuses and tissues from ZIKV-exposed fetuses treated with ZIKV-specific and negative control probes, respectively, had no staining. Red arrowheads indicate regions with ZIKV RNA. (c) Combined enrichment map of GO biological process terms with significant positive or negative association to treatment groups. Circles represent gene sets with the outer ring representing fetuses from the intracerebral (IC) group (G295 IC) and the inner ring representing fetuses from the intraperitoneal + intra-amniotic (IP + IA) group (G296 IP + IA). White space in the inner or outer rings indicates no significant enrichment. All nodes had a p-value of < 0.025 . The circle size is scaled to the number of genes in the gene set and colour is scaled to the p-value. The green lines indicate shared genes between the gene sets. Gene sets with either increased or decreased enrichment are in red and blue respectively. Subnetworks related to immunity are organized top right; neuro related subnetworks are bottom right; the left is cell signalling, division and metabolism subnetworks. (d) Heatmaps of the 669 genes with FDR corrected p-value < 0.05 were clusters by hierarchical clustering. Gene sets with either increased or decreased enrichment are in red or blue respectively. There was a small group of co-up-regulated genes, although with weaker expression in the IC exposed fetuses (pink highlighted group). This small set of genes was significantly enriched in a number of GO pathways related to virus, defense, immune, interferon, and stress responses (Dataset S2 – Sheet 4). G270 is a control litter. x and y axes represent, respectively, sample identification and genes. (e) A zoomed view of the co-up-regulated group (pink highlighted group in d).

detection limit. Plasma samples from the control G319 C gilt were negative for ZIKV-specific Ab at the day of parturition and 21 days later.

3.4. ZIKV Infection in Porcine Conceptuses is Associated with Impaired Health in Offspring

The control G319 C gilt delivered 8 healthy piglets, 3 mummified fetuses and one dead piglet. The G320 IC gilt delivered 4 dead, one small piglet, which died within three days, and 12 visually healthy piglets. The difference in fetal loss was not statistically different between C and IC

litters ($p = 0.29$, Fisher exact test). Interestingly, human studies on a large cohort of ZIKV infected and control pregnant women similar showed no increase in fetal loss (Brasil et al., 2016a; Rasmussen et al., 2016).

In accordance to *in utero* infection kinetics and intensity (Fig. S2; Fig. 1) and brain molecular pathology (Fig. 4) in IP + IA litters, the G321 IP + IA gilt delivered 5 small-for-gestational-age (SGA) piglets that appeared weaker than control piglets (Fig. 6) highlighted by delayed feeding start time compared to G319 C and G320 IC litters (Video S1, Video S2, and Video S3; for comparison see Video S11).

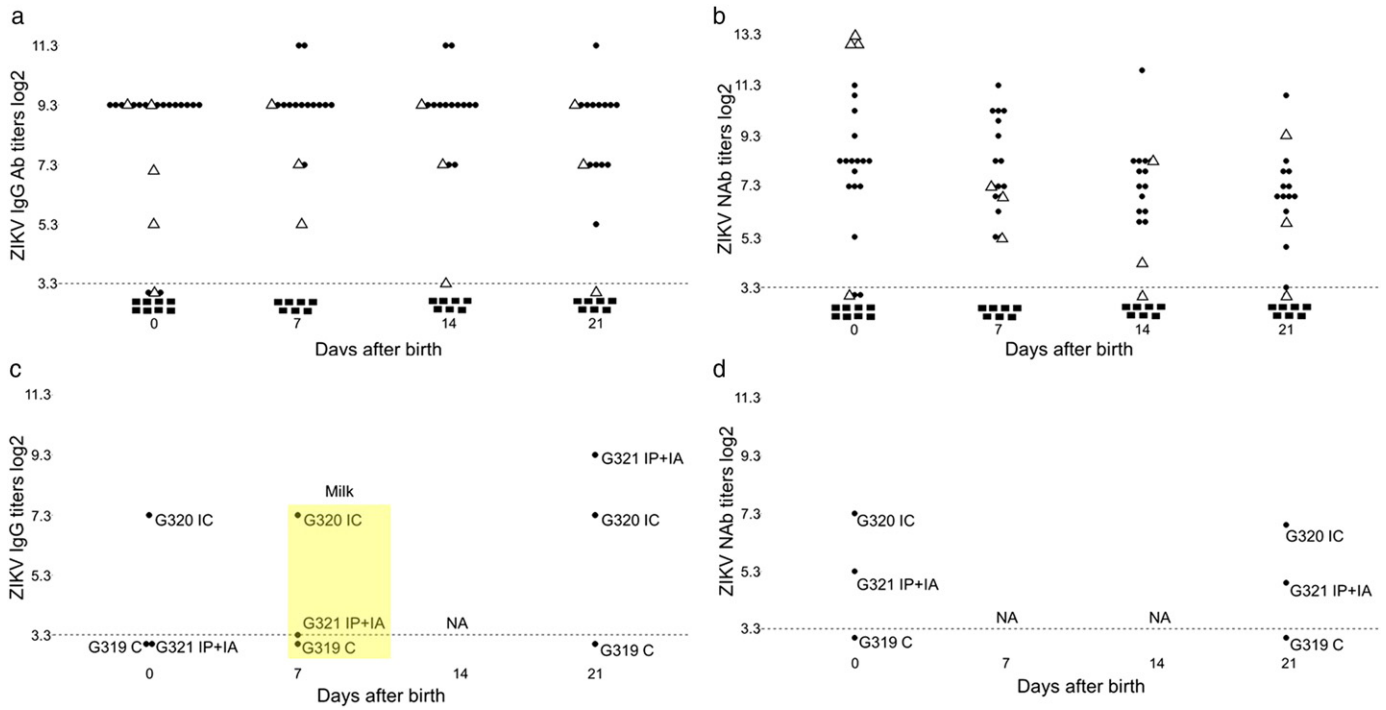


Fig. 5. ZIKV-specific Ab in offspring and mothers. Zika virus-specific IgG Ab (a) and NAb (b) titers in neonatal blood plasma. Dots represent neonates from the ZIKV-challenged G320 IC litter. Triangles represent neonates from the ZIKV-challenged G321 IP + IA litter. Quadrats represent neonates from the control G319 C litter. Zika virus-specific IgG Ab (c) and neutralizing Ab (NAb) (d) titers in maternal blood plasma and milk.

Neonatal body length and weight in the G321 IP + IA litter was significantly lower than in the G319 C litter (Fig. 6). Two piglets had possible neurological or developmental defects; newborn #100 had severe, prolonged seizure-like activity (Video S1; Video S2) and #23 had splayed back leg (Video S3). Neither neonate recovered and both were euthanized. We scanned the head of piglet #23 with MRI and CT (for control purposes piglet #3 from the control litter was euthanized and also scanned) and did not identify brain lesions (data not shown). Within three weeks, piglets in all litters gained body weight, but the IP + IA litter remained significantly smaller (Fig. 6). Neonates from the G320 IC litter also had a trend to reduced growth rate (Fig. 6). A notable exception was piglet #19, with severe wasting by the end of the study; its neutralizing ZIKV-specific Ab dropped to the detection limit at the end of the study (Fig. 5b).

Importantly, the IP + IA litter had significantly smaller brains (Fig. 6). Brain to body ratio, however, was not significantly altered (Table S5; $p = 0.09$, ANOVA on Ranks). The similar “proportionate microcephaly” has been described in human infants affected with ZIKV *in utero* (Brasil et al., 2016a).

Within 21 days, neonates from the G319 C litter remained healthy and playful (Video S4). In the G321 IP + IA litter, piglets were less active (Video S5). The worst case was piglet #24 that appeared continuously depressed and during sleep had facial seizures with an extension of the tongue. Piglet #24 deteriorated during the study and remained predominantly recumbent with continued seizure-like activities (Video S6). Interestingly, in comparison to control neonates (Video S7), neonates in the G320 IC litter had the potential increase in activity from the first days of life (Video S8). At least 8 of the 12 piglets in the G320 IC litter, both males (#13, 14, 16, 20) and females (#15, 17, 18, 22) were frequently seen to be aggressively and continually fighting during the course of the 21-day study (Video S9 and Video S10). We did not observe such extremely aggressive behavior in other litters (Video S4 and Video S5).

4. Discussion

To partially reproduce *in utero* infection in humans, we directly inoculated selected porcine conceptuses with ZIKV and characterized

infection in conceptuses and clinical outcomes in affected offspring during early life. ZIKV induced rapid trans-fetal infections, persistent infection in conceptuses, molecular pathology in fetal brains, fetal, and maternal antibody responses, and fetal *INFa* responses. Some offspring affected *in utero* were SGA, depressed, had small brains, and showed seizure-like activity. Some offspring showed potentially increased activity.

We detected robust infection in directly inoculated and non-manipulated conceptuses (Fig. S1, Fig. 1). All non-manipulated conceptuses likely acquired infection *via* a fetus-to-fetus transmission. Linear regression modeling kinetics of *in utero* infection also suggests efficient fetus-to-fetus *in utero* transmission (Fig. S2). Despite the development of maternal Ab, ZIKV was not detected in maternal blood, endometrium, and maternal uterine LN, suggesting the transit nature of maternal infection.

We identified high virus titers in fetal membranes from almost all conceptuses in IP + IA and IC litters (Fig. 1) and ZIKV in PL and AM by ISH (Fig. 2), demonstrating that ZIKV efficiently finds its way to the PL and AM independent of the exposure method. However, in IC litters PCR and infectious ZIKV titers in fetal membranes were significantly lower than in IP + IA litters (Fig. 1). The regression analysis also indicates that ZIKV passed faster from conceptus to conceptus in IP + IA litters than in IC litters (Fig. S2). Different inoculation doses, $4 \log_{10}$ TCID₅₀ per fetus in IC litters *versus* $5 \log_{10}$ TCID₅₀ per fetus in IP + IA litters, are likely responsible for differences between experimental groups. A potential co-factor for different infection kinetics is the initial delivery method. Different *in utero* infection kinetics and intensities in experimental groups might explain the distinct clinical phenotypes in IP + IA and IC litters (discussed below).

The limitation of the porcine model is epitheliochorial placentation, which can confound comprehensive modeling of ZIKV transmission in the hemochorial human placenta. However, all major cell types found in the human fetal placental mesenchyme, like Hofbauer cells, placental fibroblasts, and endothelial cells, are present in the porcine fetal placental mesenchyme (Karniyuchuk and Nauwynck, 2009; Karniyuchuk et al., 2011; Novakovic et al., 2016). The porcine allantochorion performs the same fundamental functions during pregnancy as the human placenta: gas and waste exchange, fetal nutrition and protection. Replicating in the porcine placenta, ZIKV may evoke the placental dysfunction

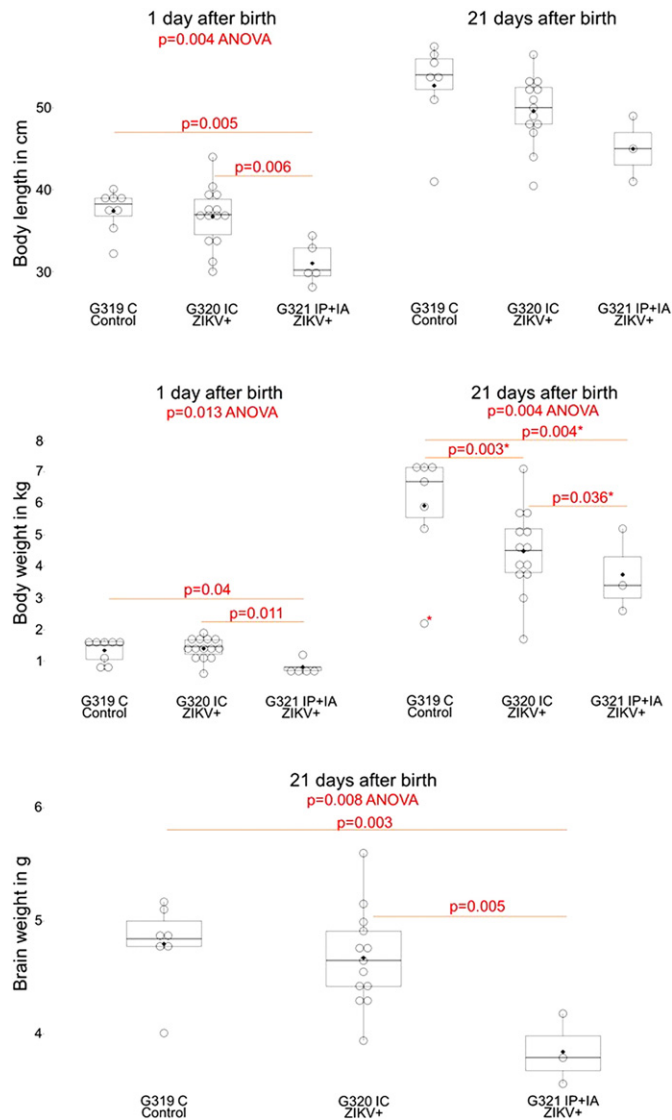


Fig. 6. Body and brain measurements in offspring exposed to ZIKV infection *in utero*. Body and brain measurements in neonates exposed *in utero* to ZIKV. G319 C – control litter; G320 IC – in this litter selected fetuses were intracerebrally inoculated *in utero* with ZIKV; G321 IP + IA – in this litter selected fetuses were intraperitoneally + intra-amniotic inoculated *in utero* with ZIKV. Body weight at 21 days was significantly different between groups if an outlier (*) was removed from analyses; otherwise, $p = 0.07$. Each box represents 25–75% of observations. Whiskers below and above each box represent the 10th and 90th percentiles. Dots represent individual piglets. The solid line and diamond within the box are median and mean, respectively. Stillborn and mummified fetuses were excluded from analyses. Difference between litters was tested by ANOVA, following by a pairwise comparison with Tukey's test.

that is partially comparable with the ZIKV-induced dysfunction in the human placenta and may similarly affect the developing conceptus. In support we observed SGA porcine neonates that may have arose from ZIKV-induced placental dysfunction and fetal growth restriction (Adibi et al., 2016).

The detection of ZIKV RNA by PCR and ISH, and molecular responses to viral infection determined by RNA-seq, suggest ZIKV infection in fetal brains at least for some period within 28 days post inoculation. We identified ZIKV in less than a half of the fetal brains tested (Fig. 4), while all conceptuses had ZIKV infection in PL and AM (Fig. 1). Reasons behind the different patterns of infection in porcine brains and fetal membranes need to be further addressed.

The altered gene expression in porcine fetal brains indicated ongoing molecular and probably functional pathology. RNA-seq analysis showed 669 significantly dysregulated genes (Dataset S2 – Sheet 1).

Among them, for example, there were genes with potential roles in migratory behavior of neural stem cells (*MMP14* (Alexiades et al., 2015)), epileptogenesis (*FN1* (Dixit et al., 2016)), and regulation of autism risk genes during cortical neurogenesis (*TBR1* (Notwell et al., 2016)). Additional studies with larger sample sizes are required to confirm findings and identify how all these molecular cascades contribute to abnormal brain development, function, and clinical phenotypes.

Piglets from the G321 IP + IA litter had significantly smaller brains (Fig. 6). Brain to body ratio, however, was not significantly altered. The similar “proportionate microcephaly” was not described in ZIKV-affected human infants (Brasil et al., 2016a). Animals, however, did not show classical microcephaly (small heads and normal-sized bodies) or brain lesions. We inoculated selected fetuses with ZIKV at mid gestation, 50 gd, exposing entire litters to infection at mid and later gestation when, similar to humans, the fetal pig brain undergoes a growth spurt (Antonson et al., 2017; Antonson et al., 2016; Dickerson and Dobbing, 1967; Dobbing and Sands, 1979; Pond et al., 2000). Human and mouse studies suggest that severe brain pathology in fetuses and neonates is a result of ZIKV infection during early embryonic and fetal development (França et al., 2016; Melo et al., 2016; Vermillion et al., 2017; Xavier-Neto et al., 2017). Our assumption is that ZIKV will cause more severe brain infection and pathology after inoculation of pig conceptuses early during development. If our assumption is correct, having the comparable brain development in pigs and humans (Dickerson and Dobbing, 1966; Gieling et al., 2011; Glauser, 1966; Lind et al., 2007; Lunney, 2007; Thibault and Margulies, 1998), the porcine model can become a valuable tool to study ZIKV-induced brain pathology at early congenital periods and probably sequelae after birth.

In accordance to distinct *in utero* infection kinetics (Fig. S2) and intensity (Fig. 1) in IP + IA and IC litters, ZIKV infection in porcine conceptuses was associated with two clinical phenotypes in offspring. The G321 IP + IA gilt delivered piglets that were SGA, with smaller than normal bodies, heads, and brains (Fig. 6), showed seizure-like activity and impaired health during early life (Video S1, S2, S5, S6). This porcine pathology is in high agreement with previous human studies where SGA phenotype was a major outcome in symptomatic neonates affected with ZIKV *in utero* (Brasil et al., 2016a; Rasmussen et al., 2016). Seizures and epilepsy are also frequent in symptomatic human neonates exposed to ZIKV *in utero* (Asadi-Pooya, 2016; Carvalho et al., 2017; Moura da Silva et al., 2016).

In contrast to depressed piglets in the IP + IA litter, piglets from the G320 IC gilt showed the potential increase in activity with continued fighting between siblings. Hyperactivity and altered behavior due to viral infection, for example, Borna disease virus infection (Solbrig et al., 1996), is known in animals. Prenatal stress, including infection during pregnancy, may lead to various behavioral phenotypes in the juvenile, adult or aged progeny, including higher emotionality and aggressiveness (Antonson et al., 2016; Atladóttir et al., 2010; Brown and Derkits, 2010; Brown, 2012; Careaga et al., 2017; Huizink et al., 2004; Jiang et al., 2016; Kranendonk et al., 2006). Also, altered behavior associated with irritability, impatient crying, and anxiety have been recently described as most common clinical symptoms in human infants exposed *in utero* to ZIKV (Moura da Silva et al., 2016).

While variation in clinical phenotypes in this study is similar to variation in clinical representations observed in humans, additional studies are warranted. We will continue to increase the sample size in subsequent experiments with standardized methods for behavioral and cognitive research (Andersen et al., 2016; Gieling et al., 2011; Kanitz et al., 2016; Lind et al., 2005; Lind et al., 2004; van der Staay et al., 2009). If confirmed and standardized, relevant clinical phenotypes will benefit testing of therapeutic interventions during pregnancy and in offspring.

The size and brain physiology of porcine fetuses are close to human fetuses providing a model to develop *in utero* delivery methods, and test safety, and efficacy of therapeutics against ZIKV. Promising *in utero* approaches to treat non-infectious diseases have been recently reported in animals (Liu et al., 2015) and humans (Götherström et al., 2014). It

is of particular interest to develop *in utero* interventions combining antiviral therapy and therapy targeting molecular neuropathology to prevent and alleviate brain defects in fetuses and offspring.

In summary, our findings demonstrate that ZIKV in porcine conceptuses causes persistent infection for at least one–two months and may impair health in offspring. The established fetal pig model can be used to test therapeutic interventions *in vivo*.

Supplementary data to this article can be found online at <https://doi.org/10.1016/j.ebiom.2017.09.021>.

Grant support

Financial support was provided by Genome Canada, Emerging Issue Program grant #418402, the Public Health Agency of Canada and the Government of Saskatchewan through Innovation Saskatchewan #418836.

Conflicts of Interest

The authors declare no competing financial interests.

Autours Contributions

U.K. conceived the study. B.C., V.G., U.K. designed experiments. C.W., D.W., S.W. performed animal experiments. J.D., K.L., M.D.-O., G.M., U.K. performed laboratory experiments. B.C. performed RNA-seq and bioinformatics. G.S., H.D. performed and analyzed CT and MRI. Y.H. histopathological analysis. A.P., M.G., D.S., B.C., V.G., U.K. data analysis and interpretation, and funding acquisition. U.K. wrote the first draft of the paper; all authors edited the manuscript.

Acknowledgment

We would like to acknowledge the VIDO-InterVac animal care personnel for the excellent assistance with animal experiments. We thank Donna Dent, Philip Dillman, Todd Reichert, and Ian Shirley for Bio-Plex cytokine assay, histology, whole slide scanning, and light microscopy. We also grateful to Jin Huang and Leanne Malec for MRI and CT scanning. ZIKV was provided by Centers for Disease Control and Prevention, Division of Vector-Borne Diseases, Fort Collins, Colorado, USA. This paper was published with the permission of the Director of VIDO-InterVac, manuscript #795.

References

- Adams Waldorf, K.M., Stencel-Baerenwald, J.E., Kapur, R.P., Studholme, C., Boldenow, E., Vornhagen, J., Baldessari, A., Dighe, M.K., Thiel, J., Merillat, S., Armistead, B., Tisoncik-Go, J., Green, R.R., Davis, M.A., Dewey, E.C., Fairgrieve, M.R., Gatenby, J.C., Richards, T., Garden, G.A., Diamond, M.S., Juul, S.E., Grant, R.F., Kuller, L., Shaw, D.W.W., Ogle, J., Gough, G.M., Lee, W., English, C., Hevner, R.F., Dobyns, W.B., Gale, M., Rajagopal, L., 2016. Fetal brain lesions after subcutaneous inoculation of Zika virus in a pregnant nonhuman primate. *Nat. Med.* <https://doi.org/10.1038/nm.4193>.
- Adibi, J.J., Marques, E.T.A., Cartus, A., Beigi, R.H., 2016. Teratogenic effects of the Zika virus and the role of the placenta. *Lancet* 387:1587–1590. [https://doi.org/10.1016/S0140-6736\(16\)00650-4](https://doi.org/10.1016/S0140-6736(16)00650-4).
- Aigner, B., Renner, S., Kessler, B., Klymiuk, N., Kurome, M., Wunsch, A., Wolf, E., 2010. Transgenic pigs as models for translational biomedical research. *J. Mol. Med. (Berl)* 88:653–664. <https://doi.org/10.1007/s00109-010-0610-9>.
- Alexiades, N.G., Auffinger, B., Kim, C.K., Hasan, T., Lee, G., Deheeger, M., Tobias, A.L., Kim, J., Balyasnikova, I., Lesniak, M.S., Aboody, K., Ahmed, A.U., 2015. MMP14 as a novel downstream target of VEGFR2 in migratory glioma-tropic neural stem cells. *Stem Cell Res.* 15:598–607. <https://doi.org/10.1016/j.scr.2015.10.005>.
- Alisky, J.M., 2006. Neurotransmitter depletion may be a cause of dementia pathology rather than an effect. *Med. Hypotheses* 67:556–560. <https://doi.org/10.1016/j.mehy.2006.02.043>.
- Amaral, A.J., Megens, H.-J., Kerstens, H.H.D., Heuven, H.C.M., Dibbitts, B., Crooijmans, R.P.M.A., den Dunnen, J.T., Groenen, M.A.M., 2009. Application of massive parallel sequencing to whole genome SNP discovery in the porcine genome. *BMC Genomics* 10: 374. <https://doi.org/10.1186/1471-2164-10-374>.
- Amstey, M.S., 1969. Intra-amniotic inoculation of rubella virus. *Am. J. Obstet. Gynecol.* 104, 573–577.
- Andersen, A.D., Sangild, P.T., Munch, S.L., van der Beek, E.M., Renes, I.B., Ginneken, C. van, Greisen, G.O., Thymann, T., 2016. Delayed growth, motor function and learning in preterm pigs during early postnatal life. *Am. J. Phys. Regul. Integr. Comp. Phys.* 310: R481–92. <https://doi.org/10.1152/ajpregu.00349.2015>.
- Antonson, A.M., Radlowski, E.C., Lawson, M.A., Rytch, J.L., Johnson, R.W., 2016. Maternal viral infection during pregnancy elicits anti-social behavior in neonatal piglet offspring independent of postnatal microglial cell activation. *Brain Behav. Immun.* <https://doi.org/10.1016/j.bbi.2016.09.019>.
- Antonson, A.M., Radlowski, E.C., Lawson, M.A., Rytch, J.L., Johnson, R.W., 2017. Maternal viral infection during pregnancy elicits anti-social behavior in neonatal piglet offspring independent of postnatal microglial cell activation. *Brain Behav. Immun.* 59: 300–312. <https://doi.org/10.1016/j.bbi.2016.09.019>.
- Asadi-Pooya, A.A., 2016. Zika virus-associated seizures. *Seizure* 43:13. <https://doi.org/10.1016/j.seizure.2016.10.011>.
- Atladóttir, H.Ó., Thorsen, P., Østergaard, L., Schendel, D.E., Lemcke, S., Abdallah, M., Parner, E.T., 2010. Maternal infection requiring hospitalization during pregnancy and autism spectrum disorders. *J. Autism Dev. Disord.* 40:1423–1430. <https://doi.org/10.1007/s10803-010-1006-y>.
- Bassols, A., Costa, C., Eckersall, P.D., Osada, J., Sabrià, J., Tibau, J., 2014. The pig as an animal model for human pathologies: A proteomics perspective. *PROTEOMICS - Clin. Appl.* 8: 715–731. <https://doi.org/10.1002/prca.201300099>.
- Bauer, R., Walter, B., Brandl, U., 2007. Intrauterine growth restriction improves cerebral O2 utilization during hypercapnic hypoxia in newborn piglets. *J. Physiol.* 584: 693–704. <https://doi.org/10.1113/jphysiol.2007.142778>.
- Baxa, M., Hruska-Plochan, M., Juhas, S., Vodicka, P., Pavlok, A., Juhasova, J., Miyahara, A., Nejime, T., Klima, J., Macakova, M., Marsala, S., Weiss, A., Kubickova, S., Musilova, P., Vrtel, R., Sontag, E.M., Thompson, L.M., Schier, J., Hansikova, H., Howland, D.S., Cattaneo, E., DiFiglia, M., Marsala, M., Motlik, J., 2013. A transgenic minipig model of Huntington's Disease. *J. Huntingtons. Dis.* 2:47–68. <https://doi.org/10.3233/JHD-130001>.
- Bayer, A., Lennemann, N.J., Ouyang, Y., Bramley, J.C., Morosky, S., Marques, E.T.D.A., Cherry, S., Sadovsky, Y., Coyne, C.B., 2016. Type III interferons produced by human placental trophoblasts confer protection against Zika virus infection. *Cell Host Microbe* 19: 705–712. <https://doi.org/10.1016/j.chom.2016.03.008>.
- Bhatnagar, J., Rabeneck, D.B., Martinez, R.B., Reagan-Steiner, S., Ermias, Y., Estetter, L.B.C., Suzuki, T., Ritter, J., Keating, M.K., Hale, G., Gary, J., Muehlenbachs, A., Lambert, A., Lanciotti, R., Odiibo, T., Meaney-Delman, D., Bolaños, F., Saad, E.A.P., Shieh, W.-J., Zaki, S.R., 2017. Zika virus RNA replication and persistence in brain and placental tissue. *Emerg. Infect. Dis.* 23. <https://doi.org/10.3201/eid2303.161499>.
- Brasil, P., Pereira, J.P., Moreira, M.E., Ribeiro Nogueira, R.M., Damasceno, L., Wakimoto, M., Rabello, R.S., Valderramos, S.G., Halai, U.-A., Salles, T.S., Zin, A.A., Horovitz, D., Daltro, P., Boechat, M., Raja Gabaglia, C., Carvalho de Sequeira, P., Pilotto, J.H., Medialdea-Carrera, R., Cotrim da Cunha, D., Abreu de Carvalho, L.M., Pone, M., Machado Siqueira, A., Calvet, G.A., Rodrigues Baião, A.E., Neves, E.S., Nassar de Carvalho, P.R., Hasue, R.H., Marschik, P.B., Einspieler, C., Janzen, C., Cherry, J.D., Bispo de Filippis, A.M., Nielsen-Saines, K., 2016a. Zika virus infection in pregnant women in Rio de Janeiro. *N. Engl. J. Med.* 375:2321–2334. <https://doi.org/10.1056/NEJMoa1602412>.
- Brasil, P., Pereira, J.P., Raja Gabaglia, C., Damasceno, L., Wakimoto, M., Ribeiro Nogueira, R.M., Carvalho de Sequeira, P., Machado Siqueira, A., Abreu de Carvalho, L.M., Cotrim da Cunha, D., Calvet, G.A., Neves, E.S., Moreira, M.E., Rodrigues Baião, A.E., Nassar de Carvalho, P.R., Janzen, C., Valderramos, S.G., Cherry, J.D., Bispo de Filippis, A.M., Nielsen-Saines, K., 2016b. Zika virus infection in pregnant women in rio de janeiro - preliminary report. *N. Engl. J. Med.* <https://doi.org/10.1056/NEJMoa1602412>.
- Brown, A.S., 2012. Epidemiologic studies of exposure to prenatal infection and risk of schizophrenia and autism. *Dev. Neurobiol.* 72:1272–1276. <https://doi.org/10.1002/dneu.22024>.
- Brown, A.S., Derkits, E.J., 2010. Prenatal infection and schizophrenia: a review of epidemiologic and translational studies. *Am. J. Psychiatry* 167:261–280. <https://doi.org/10.1176/appi.ajp.2009.09030361>.
- Burke, C., Sinclair, K., Cowin, G., Rose, S., Pat, B., Gobe, G., Colditz, P., 2006. Intrauterine growth restriction due to uteroplacental vascular insufficiency leads to increased hypoxia-induced cerebral apoptosis in newborn piglets. *Brain Res.* 1098:19–25. <https://doi.org/10.1016/j.brainres.2006.04.129>.
- Careaga, M., Murai, T., Bauman, M.D., 2017. Maternal immune activation and autism spectrum disorder: from rodents to nonhuman and human primates. *Biol. Psychiatry* 81: 391–401. <https://doi.org/10.1016/j.biopsych.2016.10.020>.
- Carvalho, M.D.C.G., Miranda-Filho, D. de B., van der Linden, V., Sobral, P.F., Ramos, R.C.F., Rocha, M.Á.W., Cordeiro, M.T., de Alencar, S.P., Nunes, M.L., 2017. Sleep EEG patterns in infants with congenital Zika virus syndrome. *Clin. Neurophysiol.* 128:204–214. <https://doi.org/10.1016/j.clinph.2016.11.004>.
- Cassetti, M.C., Durbin, A., Harris, E., Rico-Hesse, R., Roehrig, J., Rothman, A., Whitehead, S., Natarajan, R., Laughlin, C., 2010. Report of an NIAID workshop on dengue animal models. *Vaccine* 28:4229–4234. <https://doi.org/10.1016/j.vaccine.2010.04.045>.
- Chen, J., Feng, Y., Chen, L., Xiao, J., Liu, T., Yin, Z., Chen, S., 2011. Long-term impact of intrauterine MCMV infection on development of offspring nervous system. *J. Huazhong Univ. Sci. Technol. Medical Sci.* 31:371–375. <https://doi.org/10.1007/s11596-011-0383-6>.
- Collie, M.H., Rushton, D.J., Sweet, C., Hussein, R.H., Smith, H., 1982. Ferret foetal infection with influenza virus at early gestation. *Br. J. Exp. Pathol.* 63, 299–304.
- Cugola, F.R., Fernandes, I.R., Russo, F.B., Freitas, B.C., Dias, J.L.M., Guimarães, K.P., Benazzato, C., Almeida, N., Pignatari, G.C., Romero, S., Polonio, C.M., Cunha, I., Freitas, C.L., Brandão, W.N., Rossato, C., Andrade, D.G., Faria, D. de P., Garcez, A.T., Buchpiguel, C.A., Braconi, C.T., Mendes, E., Sall, A.A., Zanotto, P.M. de A., Peron, J.P.S., Muotri, A.R., Beltrão-Braga, P.C.B., 2016. The Brazilian Zika Virus Strain Causes Birth Defects in Experimental Models. *Nature Advance On.* <https://doi.org/10.1038/nature18296>.

- Cui, L., Zou, P., Chen, E., Yao, H., Zheng, H., Wang, Q., Zhu, J.-N., Jiang, S., Lu, L., Zhang, J., 2017. Visual and motor deficits in grown-up mice with congenital Zika virus infection. *EBioMedicine*. <https://doi.org/10.1016/j.ebiom.2017.04.029>.
- Darbellay, J., Lai, K., Babiuik, S., Berhane, Y., Ambagala, A., Wheler, C., Wilson, D., Walker, S., Potter, A., Gilmour, M., Safronetz, D., Gerds, V., Karniyuchuk, U., 2017. Neonatal pigs are susceptible to experimental Zika virus infection. *Emerg. Microbes Infect.* 6, e6. <https://doi.org/10.1038/em.2016.133>.
- Dickerson, J.W., Dobbing, J., 1966. Some peculiarities of cerebellar growth in pigs. *Proc. R. Soc. Med.* 59, 1088.
- Dickerson, J.W., Dobbing, J., 1967. Prenatal and postnatal growth and development of the central nervous system of the pig. *Proc. R. Soc. Lond. Ser. B Biol. Sci.* 166, 384–395.
- Dixit, A.B., Banerjee, J., Srivastava, A., Tripathi, M., Sarkar, C., Kakkur, A., Jain, M., Chandra, P.S., 2016. RNA-seq analysis of hippocampal tissues reveals novel candidate genes for drug refractory epilepsy in patients with MTLE-HS. *Genomics* 107:178–188. <https://doi.org/10.1016/j.ygeno.2016.04.001>.
- Dobbing, J., Sands, J., 1979. Comparative aspects of the brain growth spurt. *Early Hum. Dev.* 3, 79–83.
- Dohrn, N., Le, V.Q., Petersen, A., Skovbo, P., Pedersen, I.S., Ernst, A., Krarup, H., Petersen, M.B., 2015. *ECEL1* mutation causes fetal arthrogyposis multiplex congenita. *Am. J. Med. Genet. Part A* 167:731–743. <https://doi.org/10.1002/ajmg.a.37018>.
- Ferenc, K., Pietrzak, P., Godlewski, M.M., Piwowarski, J., Kiliańczyk, R., Guilloteau, P., Zabielski, R., 2014. Intrauterine growth retarded piglet as a model for humans—studies on the perinatal development of the gut structure and function. *Reprod. Biol.* 14:51–60. <https://doi.org/10.1016/j.repbio.2014.01.005>.
- França, G.V., Schuler-Faccini, L., Oliveira, W.K., Henriques, C.M., Carmo, E.H., Pedi, V.D., Nunes, M.L., Castro, M.C., Serruya, S., Silveira, M.F., Barros, F.C., V., C., 2016. Congenital Zika virus syndrome in Brazil: a case series of the first 1501 livebirths with complete investigation. *Lancet* [https://doi.org/10.1016/S0140-6736\(16\)30902-3](https://doi.org/10.1016/S0140-6736(16)30902-3).
- Gerds, V., Wilson, H.L., Meurens, F., Van Drunen Littel-Van den Hurk, S., Wilson, D., Walker, S., Wheler, C., Townsend, H., Potter, A.A., 2015. Large animal models for vaccine development and testing. *ILAR J.* 56:53–62. <https://doi.org/10.1093/ilar/ilv009>.
- Gielsing, E.T., Schuurman, T., Nordquist, R.E., van der Staay, F.J., 2011. The pig as a model animal for studying cognition and neurobehavioral disorders. *Current Topics in Behavioral Neurosciences*:pp. 359–383 https://doi.org/10.1007/7854_2010_112.
- Glauser, E.M., 1966. Advantages of piglets as experimental animals in pediatric research. *Exp. Med. Surg.* 24, 181–190.
- Gonzalez-Bulnes, A., Astiz, S., Parraguez, V.H., Garcia-Contreras, C., Vazquez-Gomez, M., 2016. Empowering translational research in fetal growth restriction: sheep and swine animal models. *Curr. Pharm. Biotechnol.* 17, 848–855 (n.d.).
- Götherström, C., Westgren, M., Shaw, S.W.S., Åström, E., Biswas, A., Byers, P.H., Mattar, C.N.Z., Graham, G.E., Taslimi, J., Ewald, U., Fisk, N.M., Yeoh, A.E.J., Lin, J.-L., Cheng, P.-J., Choolani, M., Le Blanc, K., Chan, J.K.Y., 2014. Pre- and postnatal transplantation of fetal mesenchymal stem cells in osteogenesis imperfecta: a two-center experience. *Stem Cells Transl. Med.* 3:255–264. <https://doi.org/10.5966/sctm.2013-0090>.
- Hamel, R., Dejamac, O., Wichit, S., Echcharyawat, P., Neyret, A., Luplertlop, N., Perera-Lecoin, M., Surasombatpattana, P., Taligani, L., Thomas, F., Cao-Lormeau, V.-M., Choumet, V., Briant, L., Després, P., Amara, A., Yssel, H., Missé, D., 2015. Biology of Zika virus infection in human skin cells. *J. Virol.* 89:8880–8896. <https://doi.org/10.1128/JVI.00354-15>.
- Hecht, J.T., Ester, A., Scott, A., Wise, C.A., Iovannisci, D.M., Lammer, E.J., Langlois, P.H., Blanton, S.H., 2007. NAT2 variation and idiopathic talipes equinovarus (clubfoot). *Am. J. Med. Genet. Part A* 143A:2285–2291. <https://doi.org/10.1002/ajmg.a.31927>.
- Heck, A.L., Bray, M.S., Scott, A., Blanton, S.H., Hecht, J.T., 2005. Variation in CASP10 gene is associated with idiopathic talipes equinovarus. *J. Pediatr. Orthop.* 25, 598–602 (n.d.).
- Huizink, A.C., Mulder, E.J.H., Buitelaar, J.K., 2004. Prenatal stress and risk for psychopathology: specific effects or induction of general susceptibility? *Psychol. Bull.* 130: 115–142. <https://doi.org/10.1037/0033-2909.130.1.115>.
- Ilkal, M.A., Prasanna, Y., Jacob, P.G., Geevarghese, G., Banerjee, K., 1994. Experimental studies on the susceptibility of domestic pigs to West Nile virus followed by Japanese encephalitis virus infection and vice versa. *Acta Virol.* 38, 157–161.
- Ishikawa, Y., Kozakai, T., Morita, H., Saida, K., Oka, S., Masuo, Y., 2006. Rapid detection of mycoplasma contamination in cell cultures using SYBR Green-based real-time polymerase chain reaction. *In Vitro Cell. Dev. Biol. Anim.* 42:63–69. <https://doi.org/10.1290/0505035.1>.
- Jaradeh, S., 2006. Muscle disorders affecting oral and pharyngeal swallowing. *GI Motil. on-line*. Publ. online 16 May 2006. <https://doi.org/10.1038/gimo35>.
- Jiang, H., Xu, L., Shao, L., Xia, R., Yu, Z., Ling, Z., Yang, F., Deng, M., Ruan, B., 2016. Maternal infection during pregnancy and risk of autism spectrum disorders: A systematic review and meta-analysis. *Brain Behav. Immun.* 58:165–172. <https://doi.org/10.1016/j.bbi.2016.06.005>.
- Jonsson, D.I., Ludvigsson, P., Aradhy, S., Sigurdardottir, S., Steinarsdottir, M., Hauksdottir, H., Jonsson, J.J., 2012. A de novo 1.13 Mb microdeletion in 12q13.13 associated with congenital distal arthrogyposis, intellectual disability and mild dysmorphism. *Eur. J. Med. Genet.* 55:437–440. <https://doi.org/10.1016/j.ejmg.2012.03.001>.
- Juanjua, C., Yan, F., Li, C., Haizhi, L., Ling, W., Xinrong, W., Juan, X., Tao, L., Zongzhi, Y., Suhua, C., 2011. Murine model for congenital CMV infection and hearing impairment. *Virol. J.* 8:70. <https://doi.org/10.1186/1743-422X-8-70>.
- Kanitz, E., Hameister, T., Tuchscherer, A., Tuchscherer, M., Puppe, B., 2016. Social support modulates stress-related gene expression in various brain regions of piglets. *Front. Behav. Neurosci.* 10:227. <https://doi.org/10.3389/fnbeh.2016.00227>.
- Kapogiannis, B.G., Chakhtoura, N., Hazra, R., Spong, C.Y., 2017. Bridging knowledge gaps to understand how Zika virus exposure and infection affect child development. *JAMA Pediatr.* <https://doi.org/10.1001/jamapediatrics.2017.0002>.
- Karniyuchuk, U.U., Nauwynck, H.J., 2009. Quantitative changes of sialoadhesin and CD163 positive macrophages in the implantation sites and organs of porcine embryos/fetuses during gestation. *Placenta* 30:497–500. <https://doi.org/10.1016/j.placenta.2009.03.016>.
- Karniyuchuk, U.U., Nauwynck, H.J., 2013. Pathogenesis and prevention of placental and transplacental porcine reproductive and respiratory syndrome virus infection. *Vet. Res.* 44. <https://doi.org/10.1186/1297-9716-44-95>.
- Karniyuchuk, U.U., Saha, D., Geldhof, M., Vanhee, M., Cornille, P., Van den Broeck, W., Nauwynck, H.J., 2011. Porcine reproductive and respiratory syndrome virus (PRRSV) causes apoptosis during its replication in fetal implantation sites. *Microb. Pathog.* 51. <https://doi.org/10.1016/j.micpath.2011.04.001>.
- Kragh, P.M., Nielsen, A.L., Li, J., Du, Y., Lin, L., Schmidt, M., Bøgh, I.B., Holm, I.E., Jakobsen, J.E., Johansen, M.G., Purup, S., Bolund, L., Vajta, G., Jørgensen, A.L., 2009. Hemizygous minipigs produced by random gene insertion and handmade cloning express the Alzheimer's disease-causing dominant mutation APPsw. *Transgenic Res.* 18: 545–558. <https://doi.org/10.1007/s11248-009-9245-4>.
- Kranendonk, G., Hopster, H., Fillerup, M., Ekkel, E.D., Mulder, E.J.H., Taverne, M.A.M., 2006. Cortisol administration to pregnant sows affects novelty-induced locomotion, aggressive behaviour, and blunts gender differences in their offspring. *Horm. Behav.* 49: 663–672. <https://doi.org/10.1016/j.yhbeh.2005.12.008>.
- Krauer, F., Riesen, M., Reveiz, L., Oladapo, O.T., Martínez-Vega, R., Porgo, T.V., Haefliger, A., Broutet, N.J., Low, N., WHO Zika Causality Working Group, 2017. Zika virus infection as a cause of congenital brain abnormalities and Guillain-Barré syndrome: systematic review. *PLoS Med.* 14, e1002203. <https://doi.org/10.1371/journal.pmed.1002203>.
- Larochelle, R., Antaya, M., Morin, M., Magar, R., 1999. Typing of porcine circovirus in clinical specimens by multiplex PCR. *J. Virol. Methods* 80, 69–75.
- Lazear, H.M., Govero, J., Smith, A.M., Platt, D.J., Fernandez, E., Miner, J.J., Diamond, M.S., 2016. A mouse model of Zika virus pathogenesis. *Cell Host Microbe* 19:720–730. <https://doi.org/10.1016/j.chom.2016.03.010>.
- Lefebvre, D.J., Costers, S., Van Doorselaere, J., Misinzo, G., Delputte, P.L., Nauwynck, H.J., 2008. Antigenic differences among porcine circovirus type 2 strains, as demonstrated by the use of monoclonal antibodies. *J. Gen. Virol.* 89:177–187. <https://doi.org/10.1099/vir.0.83280-0>.
- Lemke, J.R., Riesch, E., Scheurenbrand, T., Schubach, M., Wilhelm, C., Steiner, I., Hansen, J., Courage, C., Gallati, S., Bürki, S., Strozzi, S., Simonetti, B.G., Grunt, S., Steinlin, M., Alber, M., Wolff, M., Klopstock, T., Prott, E.C., Lorenz, R., Spaich, C., Rona, S., Lakshminarasimhan, M., Kröll, J., Dorn, T., Krämer, G., Synofzik, M., Becker, F., Weber, Y.G., Lerche, H., Böhm, D., Biskup, S., 2012. Targeted next generation sequencing as a diagnostic tool in epileptic disorders. *Epilepsia* 53:1387–1398. <https://doi.org/10.1111/j.1528-1167.2012.03516.x>.
- Li, C., Xu, D., Ye, Q., Hong, S., Jiang, Y., Liu, X., Zhang, N., Shi, L., Qin, C.-F., Xu, Z., 2016. Zika virus disrupts neural progenitor development and leads to microcephaly in mice. *Cell Stem Cell* <https://doi.org/10.1016/j.stem.2016.04.017>.
- Lind, N.M., Arnfred, S.M., Hemmingsen, R.P., Hansen, A.K., 2004. Prepulse inhibition of the acoustic startle reflex in pigs and its disruption by d-amphetamine. *Behav. Brain Res.* 155:217–222. <https://doi.org/10.1016/j.bbr.2004.04.014>.
- Lind, N.M., Olsen, A.K., Moustgaard, A., Jensen, S.B., Jakobsen, S., Hansen, A.K., Arnfred, S.M., Hemmingsen, R.P., Gjedde, A., Cumming, P., 2005. Mapping the amphetamine-evoked dopamine release in the brain of the Göttingen minipig. *Brain Res. Bull.* 65: 1–9. <https://doi.org/10.1016/j.brainresbull.2004.08.007>.
- Lind, N.M., Moustgaard, A., Jelsing, J., Vajta, G., Cumming, P., Hansen, A.K., 2007. The use of pigs in neuroscience: modeling brain disorders. *Neurosci. Biobehav. Rev.* 31:728–751. <https://doi.org/10.1016/j.neubiorev.2007.02.003>.
- van der Linden, V., Pessoa, A., Dobyns, W., Barkovich, A.J., Júnior, H. van der L., Filho, E.L.R., Ribeiro, E.M., Leal, M. de C., Coimbra, P.P. de A., Aragão, M. de F.V.V., Verçosa, I., Ventura, C., Ramos, R.C., Cruz, D.D.C.S., Cordeiro, M.T., Mota, V.M.R., Dott, M., Hillard, C., Moore, C.A., 2016. Description of 13 infants born during October 2015–January 2016 with congenital Zika virus infection without microcephaly at birth – Brazil. *MMWR Morb. Mortal. Wkly Rep.* 65:1343–1348. <https://doi.org/10.15585/mmwr.mm6547e2>.
- Liu, X., Hall, S.R.R., Wang, Z., Huang, H., Ghanta, S., Di Sante, M., Leri, A., Anversa, P., Perrella, M.A., 2015. Rescue of neonatal cardiac dysfunction in mice by administration of cardiac progenitor cells in utero. *Nat. Commun.* 6:8825. <https://doi.org/10.1038/ncomms9825>.
- Lunney, J.K., 2007. Advances in swine biomedical model genomics. *Int. J. Biol. Sci.* 3, 179–184.
- Mair, K.H., Sedlak, C., Käser, T., Pasternak, A., Levast, B., Gerner, W., Saalmüller, A., Summerfield, A., Gerds, V., Wilson, H.L., Meurens, F., 2014. The porcine innate immune system: an update. *Dev. Comp. Immunol.* 45:321–343. <https://doi.org/10.1016/j.dci.2014.03.022>.
- Marchi, N., Angelov, L., Masaryk, T., Fazio, V., Granata, T., Hernandez, N., Hallene, K., Diglaw, T., Franic, L., Najm, I., Janigro, D., 2007. Seizure-promoting effect of blood-brain barrier disruption. *Epilepsia* 48:732–742. <https://doi.org/10.1111/j.1528-1167.2007.00988.x>.
- Mardassi, H., Mounir, S., Dea, S., 1994. Identification of major differences in the nucleocapsid protein genes of a Québec strain and European strains of porcine reproductive and respiratory syndrome virus. *J. Gen. Virol.* 75 (Pt 3):681–685. <https://doi.org/10.1099/0022-1317-75-3-681>.
- Melo, A.S. de O., Aguiar, R.S., Amorim, M.M.R., Arruda, M.B., Melo, F. de O., Ribeiro, S.T.C., Batista, A.G.M., Ferreira, T., Dos Santos, M.P., Sampaio, V.V., Moura, S.R.M., Rabello, L.P., Gonzaga, C.E., Malinger, G., Ximenes, R., de Oliveira-Szejnfeld, P.S., Tovar-Moll, F., Chimelli, L., Silveira, P.P., Delvechio, R., Higa, L., Campanati, L., Nogueira, R.M.R., Filippis, A.M.B., Szejnfeld, J., Voloch, C.M., Ferreira, O.C., Brindeiro, R.M., Tanuri, A., 2016. Congenital Zika virus infection: beyond neonatal microcephaly. *JAMA Neurol.* 73:1407–1416. <https://doi.org/10.1001/jamaneuro.2016.3720>.
- Meurens, F., Summerfield, A., Nauwynck, H., Saif, L., Gerds, V., 2012. The pig: a model for human infectious diseases. *Trends Microbiol.* 20:50–57. <https://doi.org/10.1016/j.tim.2011.11.002>.
- Miner, J.J., Cao, B., Govero, J., Smith, A.M., Fernandez, E., Cabrera, O.H., Garber, C., Noll, M., Klein, R.S., Nogueira, K.K., Mysorekar, I.U., Diamond, M.S., 2016. Zika virus infection

- during pregnancy in mice causes placental damage and fetal demise. *Cell* <https://doi.org/10.1016/j.cell.2016.05.008>.
- Mlakar, J., Korva, M., Tul, N., Popović, M., Poljšak-Prijatelj, M., Mraz, J., Kolenc, M., Resman Rus, K., Vesnaver Vipotnik, T., Fabjan Vodusek, V., Vizjak, A., Pižem, J., Petrovec, M., Avšič Županc, T., 2016. Zika Virus associated with microcephaly. *N. Engl. J. Med.* <https://doi.org/10.1056/NEJMoa1600651>.
- Morrison, T.E., Diamond, M.S., 2017. Animal models of zika virus infection, pathogenesis, and immunity. *J. Virol.* <https://doi.org/10.1128/JVI.00009-17>.
- Moura da Silva, A.A., Ganz, J.S.S., Sousa, P. da S., Doriqui, M.J.R., Ribeiro, M.R.C., Branco, M. dos R.F.C., Queiroz, R.C. de S., Pacheco, M. de J.T., Vieira da Costa, F.R., Silva, F. de S., Simões, V.M.F., Pacheco, M.A.B., Lamy-Filho, F., Lamy, Z.C., Alves, Soares De Britto E., M. T.S., 2016. Early growth and neurologic outcomes of infants with probable congenital Zika virus syndrome. *Emerg. Infect. Dis.* <https://doi.org/10.3201/eid2211.160956>.
- Nguyen, S.M., Antony, K.M., Dudley, D.M., Kohn, S., Simmons, H.A., Wolfe, B., Salamat, M.S., Teixeira, L.B.C., Wiep, G.J., Thooft, T.H., Aliota, M.T., Weiler, A.M., Barry, G.L., Weisgrau, K.L., Vosler, L.J., Mohns, M.S., Breitbach, M.E., Stewart, L.M., Rasheed, M.N., Newman, C.M., Graham, M.E., Wieben, O.E., Turski, P.A., Johnson, K.M., Post, J., Hayes, J.M., Schultz-Darken, N., Schotzko, M.L., Eudailey, J.A., Permar, S.R., Rakasz, E.G., Mohr, E.L., Capuano, S., Tarantal, A.F., Osorio, J.E., O'Connor, S.L., Friedrich, T.C., O'Connor, D.H., Golos, T.G., 2017. Highly efficient maternal-fetal Zika virus transmission in pregnant rhesus macaques. *PLoS Pathog.* <https://doi.org/10.1371/journal.ppat.1006378>.
- Notwell, J., Heavner, W.E., Darbandi, S.F., Katzman, S., McKenna, W.L., Ortiz-Londono, C.F., Tastad, D., Eckler, M.J., Rubenstein, J.L.R., McConnell, S.K., Chen, B., Bejerano, G., 2016. TBR1 regulates autism risk genes in the developing neocortex. *Genome Res.* <https://doi.org/10.1101/gr.203612.115>.
- Novakovic, P., Harding, J.C.S., Ladinig, A., Al-Dissi, A.N., MacPhee, D.J., Detmer, S.E., 2016. Relationships of CD163 and CD169 positive cell numbers in the endometrium and fetal placenta with type 2 PRRSV RNA concentration in fetal thymus. *Vet. Res.* <https://doi.org/10.1186/s13567-016-0364-7>.
- Ochs, H.D., Morton, W.R., Kuller, L.D., Zhu, Q., Tsai, C.C., Agy, M.B., Benveniste, R.E., 1993. Intra-amniotic inoculation of pigtailed macaque (*Macaca nemestrina*) fetuses with HIV and HIV-1. *J. Med. Primatol.* <https://doi.org/10.1007/BF02721628>.
- Oliveira, D.B.L., Almeida, F.J., Durigon, E.L., Mendes, É.A., Braconi, C.T., Marchetti, I., Andreata-Santos, R., Cunha, M.P., Alves, R.P.S., Pereira, L.R., Melo, S.R., Neto, D.F.L., Mesquita, F.S., Araujo, D.B., Favoretto, S.R., Sáfiadi, M.A.P., Ferreira, L.C.S., Zanotto, P.M.A., Botosso, V.F., Berezin, E.N., 2016. Prolonged shedding of Zika Virus associated with congenital infection. *N. Engl. J. Med.* <https://doi.org/10.1056/NEJMc1607583>.
- Osuna, C.E., Lim, S.-Y., Deleage, C., Griffin, B.D., Stein, D., Schroeder, L.T., Omenge, R., Best, K., Luo, M., Hraber, P.T., Andersen-Elyard, H., Ojeda, E.F.C., Huang, S., Vanlandingham, D.L., Higgs, S., Perelson, A.S., Estes, J.D., Safronetz, D., Lewis, M.G., Whitney, J.B., 2016. Zika viral dynamics and shedding in rhesus and cynomolgus macaques. *Nat. Med.* <https://doi.org/10.1038/nm.4206>.
- Pasternak, J.A., Ng, S.H., Käser, T., Meurens, F., Wilson, H.L., 2014. Grouping Pig-Specific Responses to Mitogen with Similar Responder Animals may Facilitate the Interpretation of Results Obtained in an Out-Bred Animal Model. <https://doi.org/10.4172/2157-7560.1000242>.
- Pond, W.G., Boleman, S.L., Fiorotto, M.L., Ho, H., Knabe, D.A., Mersmann, H.J., Savell, J.W., Su, D.R., 2000. Perinatal ontogeny of brain growth in the domestic pig. *Proc. Soc. Exp. Biol. Med.* <https://doi.org/10.1006/psoc.2000.1028>.
- Prather, R.S., Shen, M., Dai, Y., 2008. Genetically modified pigs for medicine and agriculture. *Biotechnol. Genet. Eng. Rev.* [https://doi.org/10.1016/S1546-5098\(08\)00001-1](https://doi.org/10.1016/S1546-5098(08)00001-1).
- Quicke, K.M., Bowen, J.R., Johnson, E.L., McDonald, C.E., Ma, H., O'Neal, J.T., Rajakumar, A., Wrammert, J., Rimawi, B.H., Pulendran, B., Schinazi, R.F., Chakraborty, R., Suthar, M.S., 2016. Zika Virus Infects Human Placental Macrophages.
- Ramos, A.M., Crooijmans, R.P.M.A., Affara, N.A., Amaral, A.J., Archibald, A.L., Beever, J.E., Bendixen, C., Churcher, C., Clark, R., Dehais, P., Hansen, M.S., Hedegaard, J., Hu, Z.-L., Kerstens, H.H., Law, A.S., Megens, H.-J., Milan, D., Nonneman, D.J., Rohrer, G.A., Rothschild, M.F., Smith, T.P.L., Schnabel, R.D., Van Tassel, C.P., Taylor, J.F., Wiedmann, R.T., Schook, L.B., Groenen, M.A.M., 2009. Design of a high density SNP genotyping assay in the pig using SNPs identified and characterized by next generation sequencing technology. *PLoS One* <https://doi.org/10.1371/journal.pone.0006524>.
- Rasmussen, S.A., Jamieson, D.J., Honein, M.A., Petersen, L.R., 2016. Zika Virus and birth defects — reviewing the evidence for causality. *N. Engl. J. Med.* <https://doi.org/10.1056/NEJMs1604338>.
- Reed, L.J., Muench, H., 1938. A simple method of estimating fifty per cent endpoints. *Am. J. Epidemiol.* <https://doi.org/10.1093/ajep/47.3.493>.
- Retallack, H., Di Lullo, E., Arias, C., Knopp, K.A., Laurie, M.T., Sandoval-Espinosa, C., Mancía Leon, W.R., Krenčik, R., Ullian, E.M., Spatazza, J., Pollen, A.A., Mandel-Brehm, C., Nowakowski, T.J., Kriegstein, A.R., DeRisi, J.L., 2016. Zika virus cell tropism in the developing human brain and inhibition by azithromycin. *Proc. Natl. Acad. Sci. U. S. A.* <https://doi.org/10.1073/pnas.1618029113>.
- Ricklin, M.E., García-Nicolás, O., Brechbühl, D., Python, S., Zumkehr, B., Nougairède, A., Charrel, R.N., Posthaus, H., Oevermann, A., Summerfeld, A., 2016. Vector-free transmission and persistence of Japanese encephalitis virus in pigs. *Nat. Commun.* <https://doi.org/10.1038/ncomms10832>.
- Saha, D., Lefebvre, D.J., Van Doorslaere, J., Atanasova, K., Barbé, F., Geldhof, M., Karniyachuk, U.U., Nauwynck, H.J., 2010. Pathologic and virologic findings in mid-gestational porcine foetuses after experimental inoculation with PCV2a or PCV2b. *Vet. Microbiol.* <https://doi.org/10.1016/j.vetmic.2010.03.017>.
- Saha, D., Karniyachuk, U.U., Huang, L., Geldhof, M., Vanhee, M., Lefebvre, D.J., Meerts, P., Ducatelle, R., Doorslaere, J.V., Nauwynck, H.J., 2014. Unusual outcome of in utero infection and subsequent postnatal super-infection with different PCV2b strains. *Virol. Sin.* <https://doi.org/10.1007/s12250-014-3431-0>.
- Schuler-Faccini, L., Ribeiro, E.M., Feitosa, I.M.L., Horovitz, D.D.G., Cavalcanti, D.P., Pessoa, A., Doriqui, M.J.R., Neri, J.J., Neto, J.M. de P., Wanderley, H.Y.C., Cernach, M., El-Husny, A.S., Pone, M.V.S., Serao, C.L.C., Sanseverino, M.T.V., 2016. Possible association between Zika virus infection and microcephaly – Brazil, 2015. *MMWR Morb. Mortal. Wkly Rep.* <https://doi.org/10.15585/mmwr.mm6503e2>.
- Shapiro-Mendoza, C.K., Rice, M.E., Galang, R.R., Fulton, A.C., VanMaldeghem, K., Prado, M.V., Ellis, E., Anesi, M.S., Simeone, R.M., Petersen, E.E., Ellington, S.R., Jones, A.M., Williams, T., Reagan-Steiner, S., Perez-Padilla, J., Deseda, C.C., Beron, A., Tufa, A.J., Rosinger, A., Roth, N.M., Green, C., Martin, S., Lopez, C.D., deWilde, L., Goodwin, M., Pagano, H.P., Mai, C.T., Gould, C., Zaki, S., Ferrer, L.N., Davis, M.S., Lathrop, E., Polen, K., Cragan, J.D., Reynolds, M., Newsome, K.B., Huertas, M.M., Bhatnagar, J., Quiñones, A.M., Nahabedian, J.F., Adams, L., Sharp, T.M., Hancock, W.T., Rasmussen, S.A., Moore, C.A., Jamieson, D.J., Munoz-Jordan, J.L., Garstang, H., Kambui, A., Masao, C., Honein, M.A., Meaney-Delman, D., Rico, A., Phippard, A., Peterson, A.B., Pomales, A., Arth, A.C., Dawson, A., Rey, A., Figueroa, A., Sanchez, A., Robinson, B., Williams, D.B., Deep, D.L., Forbes, D.P., Ailes, E.C., Marrero, F., Fortenberry, G.Z., Razzaghi, H., Ko, J.Y., Lind, J.N., Dominguez, K.L., Clarke, K., Flores, M., Biggerstaff, M.S., Danielson, M., Molina, M., Somerville, N.J., Blumenfeld, R., Tuff, R.A., Free, R.J., Chae, S.-R., Andrist, S., Kim, S.Y., Williams, T.L., Harrington, T.A., Thomason, T., Krishnasamy, V., 2017. Pregnancy outcomes after maternal Zika virus infection during pregnancy – U.S. Territories, January 1, 2016–April 25, 2017. *MMWR Morb. Mortal. Wkly Rep.* <https://doi.org/10.15585/mmwr.mm6623e1>.
- Shyy, W., Dietz, F., Dobbs, M.B., Sheffield, V.C., Morcuende, J.A., 2009. Evaluation of CAND2 and WNT7a as candidate genes for congenital idiopathic clubfoot. *Clin. Orthop. Relat. Res.* <https://doi.org/10.1007/s11999-008-0701-x>.
- Siddharthan, V., Van Wettere, A.J., Li, R., Miao, J., Wang, Z., Morrey, J.D., Julander, J.G., 2017. Zika virus infection of adult and fetal STAT2 knock-out hamsters. *Virology* <https://doi.org/10.1016/j.virol.2017.04.013>.
- Solbrig, M.V., Koob, G.F., Fallon, J.H., Reid, S., Lipkin, W.I., 1996. Prefrontal cortex dysfunction in Borna disease virus (BDV)-infected rats. *Biol. Psychiatry* [https://doi.org/10.1016/0006-3428\(96\)00636-6](https://doi.org/10.1016/0006-3428(96)00636-6).
- van der Staay, F.J., Pouzet, B., Mahieu, M., Nordquist, R.E., Schuurman, T., 2009. The d-amphetamine-treated Göttingen miniature pig: an animal model for assessing behavioral effects of antipsychotics. *Psychopharmacology* <https://doi.org/10.1007/s00213-009-1599-z>.
- Sterzl, J., Rejnek, J., Trávníček, J., 1966. Impermeability of pig placenta for antibodies. *Folia Microbiol. (Praha)*. <https://doi.org/10.1007/BF02721628>.
- Tabata, T., Pettit, M., Puerta-Guardo, H., Michlmayr, D., Wang, C., Fang-Hoover, J., Harris, E., Pereira, L., 2016. Zika virus targets different primary human placental cells, suggesting two routes for vertical transmission. *Cell Host Microbe* <https://doi.org/10.1016/j.chom.2016.07.002>.
- Tang, W.W., Young, M.P., Mamidi, A., Regla-Nava, J.A., Kim, K., Shrestha, S., Szigeti-Buck, K., Pol, A., Van den, Lindenbach, B.D., Horvath, T.L., et al., 2016. A mouse model of zika virus sexual transmission and vaginal viral replication. *Cell Rep.* <https://doi.org/10.1016/j.celrep.2016.11.070>.
- Tayade, C., Black, G.P., Fang, Y., Croy, B.A., 2006. Differential gene expression in endometrium, endometrial lymphocytes, and trophoblasts during successful and abortive embryo implantation. *J. Immunol.* <https://doi.org/10.1189/jimmunol.176.148-156>.
- Thibault, K.L., Margulies, S.S., 1998. Age-dependent material properties of the porcine cerebrum: effect on pediatric inertial head injury criteria. *J. Biomech.* [https://doi.org/10.1016/S0021-9290\(98\)00119-1](https://doi.org/10.1016/S0021-9290(98)00119-1).
- Torales, J., Barrios, I., 2017. The Zika virus beyond microcephaly: will we face an increase in mental disorders? *Fortschr. Med.* <https://doi.org/10.1007/s00213-009-1599-z>.
- Tuggle, C.K., Wang, Y., Couture, O., 2007. Advances in swine transcriptomics. *Int. J. Biol. Sci.* <https://doi.org/10.1007/s00213-009-1599-z>.
- Vanderhaeghe, C., Dewulf, J., De Vliegher, S., Papadopoulos, G.A., de Kruijff, A., Maes, D., 2010. Longitudinal field study to assess sow level risk factors associated with stillborn piglets. *Anim. Reprod. Sci.* <https://doi.org/10.1016/j.anireprosci.2010.02.010>.
- Vermillion, M.S., Lei, J., Shabi, Y., Baxter, V.K., Crilly, N.P., McLane, M., Griffin, D.E., Pekosz, A., Klein, S.L., Burd, L., 2017. Intrauterine Zika virus infection of pregnant immunocompetent mice models transplacental transmission and adverse perinatal outcomes. *Nat. Commun.* <https://doi.org/10.1038/ncomms14575>.
- Vodička, P., Smetana, K., Dvořánková, B., Emerick, T., Xu, Y.Z., Ourednik, J., Ourednik, V., Motlík, J., 2005. The miniature pig as an animal model in biomedical research. *Ann. N. Y. Acad. Sci.* <https://doi.org/10.1196/annals.1334.015>.
- Wensvoort, G., Terpstra, C., Pol, J.M.A., ter Laak, E.A., Bloemraad, M., de Kluyver, E.P., Kragten, C., van Buiten, L., den Besten, A., Wagenaar, F., Broekhuijsen, J.M., Moonen, P.L.J.M., Zetstra, T., de Boer, E., Tibben, H.J., de Jong, M.F., Van't Veld, P., Greenland, G.J.R., van Genneep, J.A., Voets, M.T., Verheijden, J.H.M., Braamskamp, J., 1991. Mystery swine disease in the Netherlands: the isolation of Lelystad virus. *Vet. Q.* <https://doi.org/10.1080/01652176.1991.9694296>.
- Whitworth, K.M., Rowland, R.R.R., Ewen, C.L., Tribble, B.R., Kerrigan, M.A., Cino-Ozuna, A.G., Samuel, M.S., Lightner, J.E., McLaren, D.G., Mileham, A.J., Wells, K.D., Prather, R.S., 2016. Gene-edited pigs are protected from porcine reproductive and respiratory syndrome virus. *Nat. Biotechnol.* <https://doi.org/10.1038/nbt.3434>.
- Wilhelm, S., Zimmermann, P., Selbitz, H.J., Truyen, U., 2006. Real-time PCR protocol for the detection of porcine parvovirus in field samples. *J. Virol. Methods* <https://doi.org/10.1016/j.jviromet.2006.01.004>.
- Xavier-Neto, J., Carvalho, M., Pascoalino, B. dos S., Cardoso, A.C., Costa, Â.M.S., Pereira, A.H.M., Santos, L.N., Saito, Â., Marques, R.E., Smetana, J.H.C., Consonni, S.R., Bandeira, C., Costa, V.V., Bajgelman, M.C., Oliveira, P.S.L. de, Cordeiro, M.T., Gonzales Gil, L.H.V., Pauletti, B.A., Granato, D.C., Paes Leme, A.F., Freitas-Junior, L., Holanda de Freitas, C.B.M., Teixeira, M.M., Bevilacqua, E., Franchini, K., 2017. Hydrocephalus and arthrogryposis in an immunocompetent mouse model of ZIKA teratogeny: a developmental study. *PLoS Negl. Trop. Dis.* <https://doi.org/10.1371/journal.pntd.0005363>.

- Xu, M.-Y., Liu, S.-Q., Deng, C.-L., Zhang, Q.-Y., Zhang, B., 2016. Detection of Zika virus by SYBR green one-step real-time RT-PCR. *J. Virol. Methods* 236:93–97. <https://doi.org/10.1016/j.jviromet.2016.07.014>.
- Zhang, F., Hammack, C., Ogden, S.C., Cheng, Y., Lee, E.M., Wen, Z., Qian, X., Nguyen, H.N., Li, Y., Yao, B., Xu, M., Xu, T., Chen, L., Wang, Z., Feng, H., Huang, W.-K., Yoon, K.-J., Shan, C., Huang, L., Qin, Z., Christian, K.M., Shi, P.-Y., Xu, M., Xia, M., Zheng, W., Wu, H., Song, H., Tang, H., Ming, G.-L., Jin, P., 2016. Molecular signatures associated with ZIKV exposure in human cortical neural progenitors. *Nucleic Acids Res.* 44:8610–8620. <https://doi.org/10.1093/nar/gkw765>.
- Zou, J., Shi, P.-Y., 2017. Adulthood sequelae of congenital Zika virus infection in mice. *EBioMedicine* 20:11–12. <https://doi.org/10.1016/j.ebiom.2017.05.005>.
- Zucker, J., Neu, N., Chiriboga, C.A., Hinton, V.J., Leonardo, M., Sheikh, A., Thakur, K., 2017. Zika virus-associated cognitive impairment in adolescent, 2016. *Emerg. Infect. Dis.* 23:1047–1048. <https://doi.org/10.3201/eid2306.162029>.